interconnected porous hydroxyapatite ceramics combined with marrow mesenchymal cells: quantitative and three-dimensional image analysis. Cell Transplant 2004;13:367–76.
32. Kaito T, Myoui A, Takaoka K, Saito N, Nishikawa M, Tamai N, *et al.* Potentiation of the activity of bone morphogenetic protein-2 in bone regeneration by a PLA–PEG/hydroxyapatite composite. Biomaterials 2005;26:73–9.
33. Akita S, Tamai N, Myoui A, Nishikawa M, Kaito T, Takaoka K, *et al.* Capillary vessel network integration by inserting a vascular pedicle enhances bone formation in tissue-engineered bone using interconnected porous hydroxyapatite ceramics. Tissue Eng 2004;10:789–95.
34. Wei X, Gao J, Messner K. Maturation-dependent repair of untreated osteochondral defects in the rabbit knee joint. J Biomed Mater Res 1997;34:63–72.
35. Kumagai K, Saito T, Koshino T. Articular cartilage repair of rabbit chondral defect: promoted by creation of periarticular bony defect. J Orthop Sci 2003;8: 700–6.
36. Schaefer D, Martin I, Jundt G, Seidel J, Heberer M, Grodzinsky A, *et al.* Tissue-engineered composites for the repair of large osteochondral defects. Arthritis Rheum 2002;46:2524–34.
37. Ikeuchi M, Dohi Y, Horiuchi K, Ohgushi H, Noshi T, Yoshikawa T, *et al.* Recombinant human bone morphogenetic protein-2 promotes osteogenesis within atelopeptide type I collagen solution by combination with rat cultured marrow cells. J Biomed Mater Res 2002;60:61–9.
38. Hegyi L, Gannon FH, Glaser DL, Shore EM, Kaplan FS, Shanahan CM. Stromal cells of fibrodysplasia ossificans progressiva lesions express smooth muscle lineage markers and the osteogenic transcription factor Runx2/Cbfa-1: clues to a vascular origin of heterotopic ossification? J Pathol 2003;201:141–8.
39. Wakitani S, Imoto K, Yamamoto T, Saito M, Murata N, Yoneda M. Human autologous culture expanded bone marrow mesenchymal cell transplantation for repair of cartilage defects in osteoarthritic knees. Osteoarthritis Cartilage 2002;10:199–206.
40. Cook SD, Patron LP, Salkeld SL, Rueger DC. Repair of articular cartilage defects with osteogenic protein-1 (BMP-7) in dogs. J Bone Joint Surg Am 2003;85-A: 116–23.
41. Sellers RS, Peluso D, Morris EA. The effect of recombinant human bone morphogenetic protein-2 (rhBMP-2) on the healing of full-thickness defects of articular cartilage. J Bone Joint Surg Am 1997;79: 1452–63.
42. Hidaka C, Goodrich LR, Chen CT, Warren RF, Crystal RG, Nixon AJ. Acceleration of cartilage repair by genetically modified chondrocytes over expressing bone morphogenetic protein-7. J Orthop Res 2003;21: 573–83.
43. Sellers RS, Zhang R, Glasson SS, Kim HD, Peluso D, D'Augusta DA, *et al.* Repair of articular cartilage defects one year after treatment with recombinant human bone morphogenetic protein-2 (rhBMP-2). J Bone Joint Surg Am 2000;82:151–61.
44. Hunziker EB, Driesang IM, Morris EA. Chondrogenesis in cartilage repair is induced by members of the transforming growth factor-beta superfamily. Clin Orthop 2001;391S:171–81.
45. Frenkel SR, Saadeh PB, Mehrara BJ, Chin GS, Steinbrech DS, Brent B, *et al.* Transforming growth factor beta superfamily members: role in cartilage modeling. Plast Reconstr Surg 2000;105:980–90.
46. Kim HD, Valentini RF. Retention and activity of BMP-2 in hyaluronic acid-based scaffolds *in vitro.* J Biomed Mater Res 2002;59:573–84.
47. Inada M, Yasui T, Nomura S, Miyake S, Deguchi K, Himeno M, *et al.* Maturational disturbance of chondrocytes in Cbfa1-deficient mice. Dev Dyn 1999;214: 279–90.
48. Otto F, Thornell AP, Crompton T, Denzel A, Gilmour KC, Rosewell IR, *et al.* Cbfa1, a candidate gene for cleidocranial dysplasia syndrome, is essential for osteoblastic differentiation and bone development. Cell 1997;89:765–71.
49. de Crombrugghe B, Lefebvre V, Nakashima K. Regulatory mechanisms in the pathways of cartilage and bone formation. Curr Opin Cell Biol 2001;13:721–7.
50. Stricker S, Fundele R, Vortkamp A, Mundlos S. Role of Runx genes in chondrocyte differentiation. Dev Biol 2002;245:95–108.
51. Kim IS, Otto F, Zabel B, Mundlos S. Regulation of chondrocyte differentiation by Cbfa1. Mech Dev 1999; 80:159–70.
52. Lodie TA, Blickarz CE, Devarakonda TJ, He C, Dash AB, Clarke J, *et al.* Systematic analysis of reportedly distinct populations of multipotent bone marrow-derived stem cells reveals a lack of distinction. Tissue Eng 2002;8: 739–51.
53. De Ugarte DA, Alfonso Z, Zuk PA, Elbarbary A, Zhu M, Ashjian P, *et al.* Differential expression of stem cell mobilization-associated molecules on multi-lineage cells from adipose tissue and bone marrow. Immunol Lett 2003;89:267–70.
54. Shapiro F, Koide S, Glimcher MJ. Cell origin and differentiation in the repair of full-thickness defects of articular cartilage. J Bone Joint Surg Am 1993;75: 532–53.
55. Langer R. Drug delivery and targeting. Nature 1998; 392:5–10.
56. Jeong B, Bae YH, Lee DS, Kim SW. Biodegradable block copolymers as injectable drug-delivery systems. Nature 1997;388:860–2.

ARTHRITIS & RHEUMATISM
Vol. 52, No. 12, December 2005, pp 3819–3828
DOI 10.1002/art.21425

Nurse-like Cells From Patients With Rheumatoid Arthritis Support the Survival of Osteoclast Precursors Via Macrophage Colony-Stimulating Factor Production

Hideki Tsuboi,[1] Nobuyuki Udagawa,[2] Jun Hashimoto,[1] Hideki Yoshikawa,[1] Naoyuki Takahashi,[2] and Takahiro Ochi[3]

Objective. **To elucidate the role of nurse-like cells (NLCs) obtained from rheumatoid arthritis (RA) patients in bone loss during progressive synovial expansion.**

Methods. **CD14+ monocytes were cocultured with NLCs for 4 weeks and collected as NLC-supported CD14+ (NCD14+) monocytes. To determine their ability to differentiate into osteoclasts, NCD14+ monocytes were further cultured with macrophage colony-stimulating factor (M-CSF) together with RANKL or tumor necrosis factor α (TNFα). NCD14+ monocytes were also cocultured with SaOS-4/3 cells, which were shown to support osteoclastogenesis in response to parathyroid hormone (PTH). CD14+ monocytes were cocultured with SaOS-4/3 cells to elucidate how SaOS-4/3 cells and NLCs supported CD14+ monocytes for a long period. Synovial expansion adjacent to bone in RA patients was examined immunohistochemically to detect osteoclast precursors such as NCD14+ monocytes.**

Results. **NLCs supported the survival of CD14+ monocytes for 4 weeks. NCD14+ as well as CD14+ monocytes differentiated into osteoclasts in the presence of M-CSF together with RANKL or TNFα. NCD14+ monocytes also differentiated into osteoclasts in PTH-treated cocultures with SaOS-4/3 cells. SaOS-4/3 cells supported the survival of CD14+ monocytes for 4 weeks in the presence, but not absence, of PTH. Treatment of SaOS-4/3 cells with PTH up-regulated the expression of M-CSF messenger RNA. Neutralizing antibodies against M-CSF inhibited the NLC-supported survival of CD14+ monocytes. CD68+ monocytes and M-CSF+ fibroblast-like synoviocytes were colocalized in regions adjacent to the destroyed bone of RA patients.**

Conclusion. **Our findings suggest that NLCs are involved in RA-induced bone destruction by maintaining osteoclast precursors via production of M-CSF.**

Osteoclasts, the multinucleated cells that resorb bone, originate from the monocyte/macrophage lineage. Recent studies have established that bone-forming osteoblasts (or, bone marrow–derived stromal cells) are involved in the differentiation and function of osteoclasts (1–4). Macrophage colony-stimulating factor (M-CSF), which is produced by osteoblasts, is an essential cytokine for osteoclast formation. Osteoblasts also express RANKL, another cytokine involved in osteoclast differentiation, as a membrane-associated cytokine. Osteoclast precursors express RANK (the receptor for RANKL), recognize RANKL expressed by osteoblasts through cell–cell interaction, and differentiate into osteoclasts in the presence of M-CSF (1–4). Osteoprotegerin (OPG), which is produced mainly by osteoblasts, is a soluble decoy receptor for RANKL and blocks osteoclastogenesis by inhibiting RANKL–RANK interactions (5,6). Bone resorption–stimulating hormones and cytokines enhance the expression of RANKL in osteoblasts. Recent studies have shown that tumor necrosis factor α (TNFα) stimulates osteoclast differentiation in the presence of M-CSF through a mechanism independent of the RANKL/RANK system (7) and that

Supported in part by a grant-in-aid from the Health Science Research grant from the Ministry of Health and Welfare of Japan.

[1]Hideki Tsuboi, MD, PhD, Jun Hashimoto, MD, PhD, Hideki Yoshikawa, MD, PhD: Osaka University Graduate School of Medicine, Suita, Japan; [2]Nobuyuki Udagawa, DDS, PhD, Naoyuki Takahashi, PhD: Matsumoto Dental University, Shiojiri, Japan; [3]Takahiro Ochi, MD, PhD: Osaka University Graduate School of Medicine, Suita, and National Hospital Organization, Sagamihara National Hospital, Sagamihara, Japan.

Address correspondence and reprint requests to Takahiro Ochi, MD, PhD, National Hospital Organization Sagamihara National Hospital, 18-1 Sakuradai, Sagamihara, Kanagawa 228-8522, Japan. E-mail: t-ochi@sagamihara-hosp.gr.jp.

Submitted for publication December 1, 2004; accepted in revised form August 18, 2005.

interleukin-1 (IL-1) acts directly on osteoclasts to induce bone-resorbing activity (8).

Rheumatoid arthritis (RA) is a chronic inflammatory disease characterized by arthritis affecting multiple joints and the progressive destruction of cartilage and bone (9). Osteoclasts activated by inflammatory cytokines are involved in bone destruction in RA. Recent studies have suggested that a progressive synovial expansion called pannus at sites of bone destruction plays important roles in osteoclastic bone resorption (10–12). In addition, osteoclasts formed from circulating precursors obtained from patients with RA have an increased bone-resorbing activity compared with those obtained from normal control subjects (13). However, the etiology of RA and the mechanism of bone destruction induced by RA have not yet been elucidated completely.

Nurse cells were first recognized in cell suspensions of dissociated thymus (14). Thymic nurse cells supported the differentiation and maturation of T cells. When bone marrow–derived T cell precursors were cocultured with thymic nurse cells, the T cell precursors crawled beneath the thymic nurse cell layers and differentiated into mature thymocytes. This phenomenon, known as pseudoemperipolesis, is peculiar to nurse cells and has been used to identify nurse-like cells (NLCs) in various tissues (15–17). We have established NLC lines from the synovium and bone marrow of patients with RA (16,17). NLCs showed characteristics similar to those of fibroblast-like synoviocytes. NLCs promoted the activation and differentiation of both B and T lymphocytes in coculture. It was also shown that stromal cell–derived factor 1 and CD106 (vascular cell adhesion molecule 1) were involved in the formation and maintenance of B cell pseudoemperipolesis by RA fibroblast-like synoviocytes (18).

We recently showed that NLCs promoted the survival of peripheral blood monocytes as well as B cells (19). Monocytes supported by NLCs possessed tartrate-resistant acid phosphatase (TRAP; a marker enzyme of osteoclasts) activity and differentiated into osteoclast-like multinucleated cells in response to some cytokines, including RANKL. However, it is not clear how fibroblast-like synoviocytes are involved in bone destruction in RA. In the present study, we examined the ability of monocytes supported for 4 weeks by NLCs to differentiate into osteoclasts in comparison with the ability of freshly isolated peripheral blood monocytes to do so. We also examined how NLCs support the survival of osteoclast precursors for a long period of culture.

MATERIALS AND METHODS

Chemicals. Recombinant human M-CSF (Leukoprol) was obtained from Kyowa Hakko Kogyo (Tokyo, Japan), recombinant soluble RANKL and OPG from PeproTech (London, UK), and recombinant human TNFα and neutralizing antibody against human M-CSF from Genzyme (Minneapolis, MN). We purchased 1α,25-dihydroxyvitamin D_3 (1α,25$[OH]_2D_3$) and prostaglandin E_2 (PGE_2) from Wako (Osaka, Japan). Human parathyroid hormone 1–34 (PTH 1–34) was obtained from Peptide Institute (Osaka, Japan). A monoclonal antibody against vitronectin receptors (VNRs; human CD51/61 complex) (23C6) was purchased from Serotec (Oxford, UK). A monoclonal antibody against human CD68 (KP1) and polyclonal antibodies against human M-CSF were from Dako (Glostrup, Denmark) and Santa Cruz Biotechnology (Santa Cruz, CA), respectively.

Cells and the coculture system. CD14+ monocytes were isolated from peripheral blood using anti-CD14 antibody–coated beads, as described previously (19). NLCs were established from synovium and bone marrow obtained from patients with RA. NLCs were cultured in Dulbecco's modified Eagle's medium (DMEM; Gibco BRL, Gaithersburg, MD) supplemented with 10% fetal calf serum (FCS; Hyclone, Logan, UT). Half of the medium was replaced weekly with the fresh medium. SaOS-4/3 cells were established from the SaOS-2 human osteosarcoma cell line by transfection with human PTH/PTH-related protein receptor complementary DNA (cDNA) (20). SaOS-4/3 cells support human osteoclast formation in response to PTH in cocultures with human peripheral blood mononuclear cells (20,21).

CD14+ monocytes (5×10^5 cells/well) were cocultured with NLCs (4×10^4 cells/well) or with SaOS-4/3 cells (4×10^4 cells/well) in the presence or absence of PTH ($10^{-8}M$) for 4 weeks in DMEM supplemented with 10% FCS in 12-well plates. Neutralizing antibodies against human M-CSF (final concentrations 50 ng/ml, 500 ng/ml, and 5,000 ng/ml) were added to some cocultures with NLCs. The culture medium was replaced every 3 days with the fresh medium. The number of CD14+ monocytes recovered from the coculture with NLCs or SaOS-4/3 cells was counted every week. After coculture for 4 weeks, the floating or weakly adherent CD14+ monocytes were harvested as NLC-supported CD14+ cells, or NCD14+ monocytes, by gently washing the culture with DMEM supplemented with 10% FCS. The ability of NCD14+ monocytes and CD14+ monocytes to differentiate into osteoclasts was compared as described below.

Osteoclast formation assay. NCD14+ monocytes (1×10^4/well) and freshly isolated CD14+ monocytes (3×10^4/well) were cultured in the presence or absence of M-CSF (25 ng/ml), RANKL (40 ng/ml), TNFα (20 ng/ml), or OPG (100 ng/ml) in α-minimum essential medium (α-MEM; Gibco) supplemented with 10% FCS in a 96-well plate. NCD14+ monocytes (2×10^4/well) were also cocultured with SaOS-4/3 cells (1×10^4/well) in 48-well plates in α-MEM supplemented with 10% FCS in the presence or absence of PTH ($10^{-8}M$). Some cultures were treated with OPG (100 ng/ml). After a specific period of time, cells were fixed and stained for TRAP using a TRAP staining kit obtained from Hokudo (Hokkaido, Japan).

For immunohistochemical staining, cells were fixed with cold methanol:acetone (50:50 volume/volume) for 10

Table 1. Sequences of polymerase chain reaction primers*

	Primers (5′–3′)		
	Sense	Antisense	Expected product size, bp
CD14	TCCCCACAAGTTCCCGGCCATC	TCCACCTCGGGCAGCTCGTCAG	315
CD68	TTCCCCCACGCAGCAAAGTGGA	ACCCCAAACCCCCTCAGTGCCC	362
CTR	TCCATGGACCTGTCATGGCGGC	TTGGCGCTTCACGGTGGTTTGG	314
M-CSF	GCTTTGCTGAATGCTCCAGC	CAGAGGGACATTGGACAAACG	308, 1,201
OPG	CCGCCTCCAAGCCCCTGAGGTT	ACACGCGGTTGTGGGTGCGATT	400
RANK	CTTCGCGTCTGTGGCCCTGGTG	CCTGGCATCTTCGCCTTGTGCG	319
RANKL	GCATGGCCCCAACGGTACACGA	TCAGCTGCGAAGGGGCACATGA	237
TNFRI	TTCTTGCCCCCACCCGTCCATC	CCAGCCATCCAGGGCCACCTTC	359
GAPDH	TGCTCTTGCTGGGGCTGGTGGT	TGCCAAGGCTGTGGGCAAGGTC	400

* CTR = calcitonin receptor; M-CSF = macrophage colony-stimulating factor; OPG = osteoprotegerin; TNFRI = tumor necrosis factor receptor I.

minutes and incubated with a monoclonal antibody against VNR, an osteoclast-associated antigen. The bound antibodies were visualized with biotinylated secondary antibodies, avidin–biotin–conjugated peroxidase, and an aminoethylcarbazole substrate kit (Histofine; Nichirei, Tokyo, Japan).

For the pit-formation assay, NCD14+ and CD14+ monocytes were cultured on dentin slices in α-MEM supplemented with 10% FCS in 48-well plates (1 slice/well) in the presence or absence of several of the factors described above. After 21 days, dentin slices were stained with Mayer's hematoxylin solution to detect resorption pits.

Reverse transcription–polymerase chain reaction (RT-PCR) analysis. Total RNA was extracted from CD14+ (5×10^6 cells) and NCD14+ (5×10^5 cells) monocytes using an RNeasy Mini kit (Qiagen, Hilden, Germany) according to the manufacturer's directions. After treatment with DNase I (Life Technologies, Rockville, MD), single-stranded cDNA was synthesized using 2 μg of each RNA sample, 100 ng of random primers, and 4 units of Omniscript reverse transcriptase (Qiagen) in a total reaction volume of 20 μl. Amplification was performed with 0.5 units of Ex *Taq* (Takara, Shiga, Japan) in a total reaction volume of 20 μl containing 1× reaction buffer, 200 μ*M* of each dNTP, and 10 pmoles of each primer. The PCR conditions were as follows: initial denaturation for 2 minutes at 94°C, then 30 cycles of 30 seconds each at 94°C and 72°C (annealing at 72°C).

To determine the expression of calcitonin receptor (CTR) messenger RNA (mRNA), NCD14+ monocytes (4×10^5/well) were cocultured with SaOS-4/3 cells (2×10^5/well) in 6-well plates with or without PTH (10^{-8}*M*) and with or without PTH (10^{-8}*M*) plus OPG (100 ng/ml). Total RNA extracted from the coculture was subjected to RT-PCR analysis of CTR mRNA expression.

To determine the expression of RANKL, OPG, and M-CSF mRNA, NLCs (5×10^6/dish) or SaOS-4/3 cells (5×10^6/dish) were cultured for 3 days in a 10-cm culture dish in the presence or absence of PTH (10^{-8}*M*), PGE_2 (10^{-6}*M*), or $1\alpha,25(OH)_2D_3$ (10^{-8}*M*). Total RNA was then extracted from the cells and subjected to a RT-PCR analysis of RANKL, OPG, and M-CSF mRNA expression.

A fragment of GAPDH cDNA was amplified as a control in all reactions. Aliquots of the PCR products were subjected to electrophoresis on 1.5% agarose gels and visualized by staining with ethidium bromide. In all cases, reproducibility was confirmed in triplicate experiments. The primer sets for CD14, CD68, CTR, M-CSF, OPG, RANK, RANKL, TNF receptor I (TNFRI), and GAPDH are shown in Table 1.

Immunohistochemical and TRAP staining of tissue samples from RA patients. Tissue samples, including the bone–synovium interface, were obtained during total knee arthroplasty in 5 RA patients, after they provided informed consent. The American College of Rheumatology (formerly, the American Rheumatism Association) criteria were used for the diagnosis of RA (22). The clinical features of the RA patients are summarized in Table 2.

Tissue samples were fixed in 4% paraformaldehyde at 4°C for 24 hours and decalcified in 20% EDTA for 2 hours in a microwave oven (H2800 Microwave Processor; Energy Beam Sciences, Agawam, MA) at 50°C and then for 22 hours at 4°C (23). Next, the samples were dehydrated through an ethanol series and embedded in paraffin. Sections (4 μm thick) were cut with a microtome and stained with TRAP and immunohistochemical stains. Immunohistochemical staining was performed by the streptavidin–biotin–peroxidase complex technique using a Histofine SAB-PO kit (Nichirei) according to the manufacturer's instructions. Briefly, after blocking endogenous peroxidase and nonspecific antigens, tissue sections were incu-

Table 2. Characteristics of the rheumatoid arthritis patients at the time of surgery*

No. of men/women	0/5
Age, mean (range) years	62.2 (57–68)
CRP, mean (range) mg/dl	1.76 (0.9–4.4)
Disease duration, mean (range) years	20.8 (14–28)
No. taking NSAIDs	5
Treatment during previous 6 months, no. of patients	
Gold salts	0
Bucillamine	0
Methotrexate	4
Prednisolone	3

* CRP = C-reactive protein; NSAIDs = nonsteroidal antiinflammatory drugs.

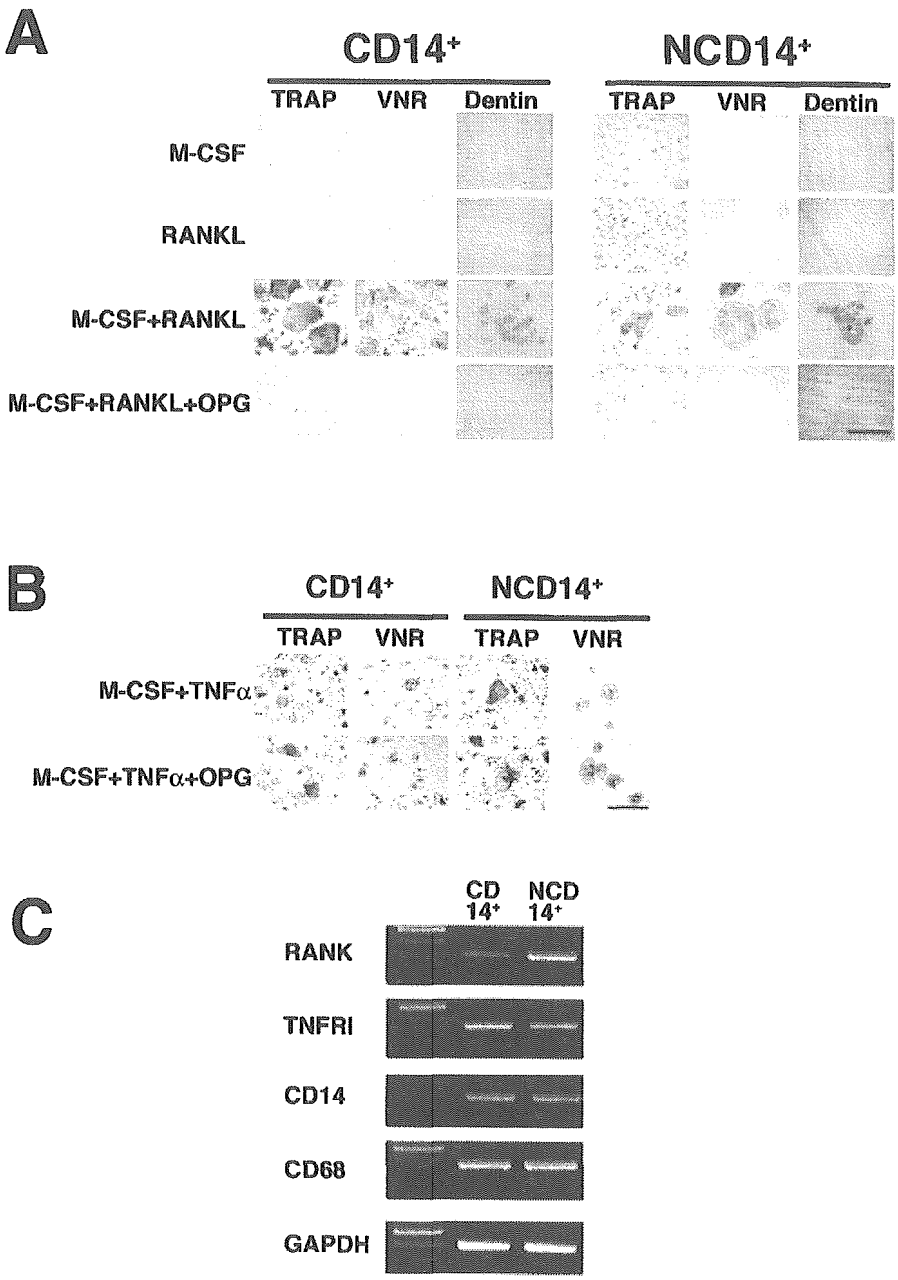

Figure 1. Osteoclast formation from CD14+ monocytes and nurse-like cell–supported CD14+ (NCD14+) monocytes. **A,** CD14+ monocytes were cultured for 7 days with or without macrophage colony-stimulating factor (M-CSF; 25 ng/ml), RANKL (40 ng/ml), M-CSF (25 ng/ml) plus RANKL (40 ng/ml), or M-CSF (25 ng/ml) plus RANKL (40 ng/ml) plus osteoprotegerin (OPG; 100 ng/ml). NCD14+ monocytes were similarly cultured for 14 days. Cultures were then fixed and stained for tartrate-resistant acid phosphatase (TRAP) or for vitronectin receptor (VNR). For the pit-formation assay, NCD14+ and CD14+ monocytes were cultured on dentin slices in the presence or absence of several of the factors described above. After 21 days in culture, dentin slices were stained with Mayer's hematoxylin to detect resorption pits. Bar = 100 μm. **B,** CD14+ and NCD14+ monocytes were cultured for 7 and 14 days, respectively, with M-CSF (25 ng/ml) plus tumor necrosis factor α (TNFα; 20 ng/ml) in the presence or absence of OPG (100 ng/ml). Cultures were stained for TRAP or VNR. Bar = 100 μm. **C,** Total RNA was extracted from CD14+ and NCD14+ monocytes, and the expression of mRNA for RANK, TNF receptor I (TNFRI), CD14, CD68, and GAPDH was analyzed by reverse transcription–polymerase chain reaction.

bated with primary antibodies against M-CSF and CD68 for 24 hours at 4°C. The sections were washed with phosphate buffered saline and incubated with the secondary antibody, followed by peroxidase-conjugated streptavidin (Nichirei). After a wash with phosphate buffered saline, the sections were incubated with 3,3′-diaminobenzidine tetrahydrochloride (Dojindo, Kumamoto, Japan) to detect peroxidase activity and then counterstained with hematoxylin. TRAP was detected using a TRAP staining kit (Hokudo).

Statistical analysis. The statistical significance of differences was analyzed using Student's *t*-test. *P* values less than 0.05 were considered significant. All results are representative of at least 3 individual experiments.

RESULTS

Cytokine-induced osteoclast formation from CD14+ and NCD14+ monocytes. CD14+ monocytes were prepared from peripheral blood, and NCD14+ monocytes were prepared from CD14+ monocytes and NLCs that had been cocultured for 4 weeks. CD14+ monocytes were cultured for 7 days with or without M-CSF, RANKL, M-CSF plus RANKL, or M-CSF plus RANKL plus OPG. Multinucleated cells positive for both TRAP and VNR were formed in the presence of M-CSF plus RANKL (Figure 1A). When CD14+ monocytes were cultured on dentin slices, resorption pits on the slices were observed only in the culture treated with M-CSF plus RANKL. Addition of OPG, a decoy receptor for RANKL, to the CD14+ culture treated with M-CSF plus RANKL inhibited the formation of TRAP+ and VNR+ multinucleated cells. Pit formation on dentin slices induced by M-CSF plus RANKL was inhibited by the addition of OPG to the CD14+ culture.

Similarly, NCD14+ monocytes differentiated into TRAP+ and VNR+ multinucleated cells in response to M-CSF plus RANKL (Figure 1A). The formation of TRAP+ and VNR+ multinucleated cells from NCD14+ monocytes was completely inhibited by the addition of OPG. However, a longer culture period was required to induce the multinucleated cells in NCD14+ cultures (7–14 days) than to induce them in CD14+ cultures (7 days). Resorption pits were also detected on dentin slices on which NCD14+ monocytes had been cultured in the presence of M-CSF plus RANKL.

Both CD14+ and NCD14+ monocytes differentiated into TRAP+ and VNR+ multinucleated cells in response to TNFα instead of RANKL in the presence of M-CSF (Figure 1B). OPG failed to inhibit the formation of TNFα-induced TRAP+ and VNR+ multinucleated cells in CD14+ and NCD14+ cultures. RT-PCR analysis showed that CD14+ and NCD14+ monocytes expressed similar levels of mRNA for the monocyte/macrophage-associated antigens CD14 and CD68 (Figure 1C). Both cell populations expressed mRNA for RANK (the receptor for RANKL) and TNFRI (the type I TNF receptor).

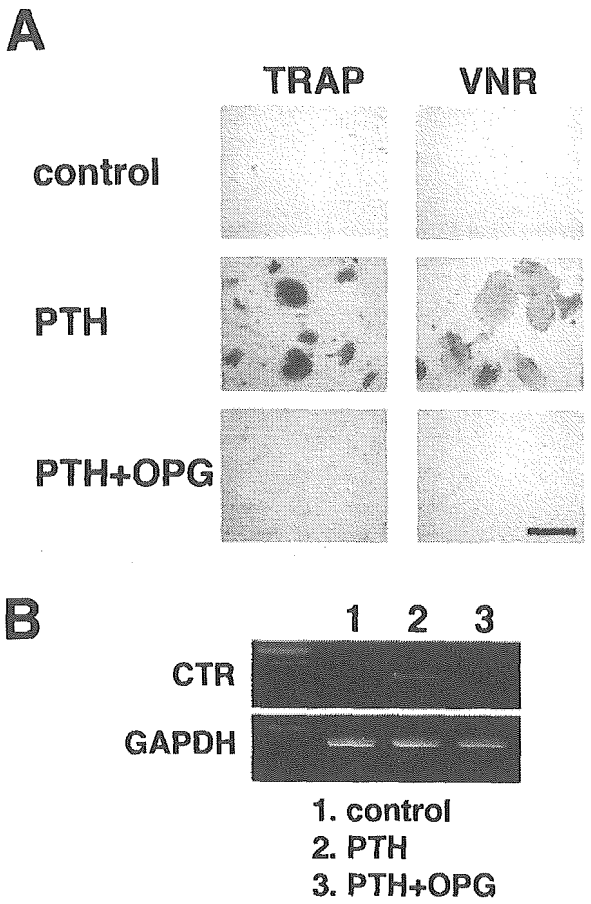

Figure 2. Osteoclast formation from nurse-like cell–supported CD14+ (NCD14+) monocytes in coculture with SaOS-4/3 cells. **A,** NCD14+ monocytes were cocultured with SaOS-4/3 cells in the presence or absence of parathyroid hormone (PTH; $10^{-8}M$). Osteoprotegerin (OPG; 100 ng/ml) was added to some cocultures treated with PTH. After 14 days, cells were fixed and stained for tartrate-resistant acid phosphatase (TRAP) or vitronectin receptor (VNR). Bar = 100 μm. **B,** NCD14+ monocytes and SaOS-4/3 cells were cocultured for 14 days with vehicle (control) (lane 1), PTH ($10^{-8}M$) (lane 2), and PTH ($10^{-8}M$) plus OPG (100 ng/ml) (lane 3). Total RNA was extracted from the cocultures, and the expression of mRNA for calcitonin receptor (CTR) and GAPDH was analyzed by reverse transcription–polymerase chain reaction.

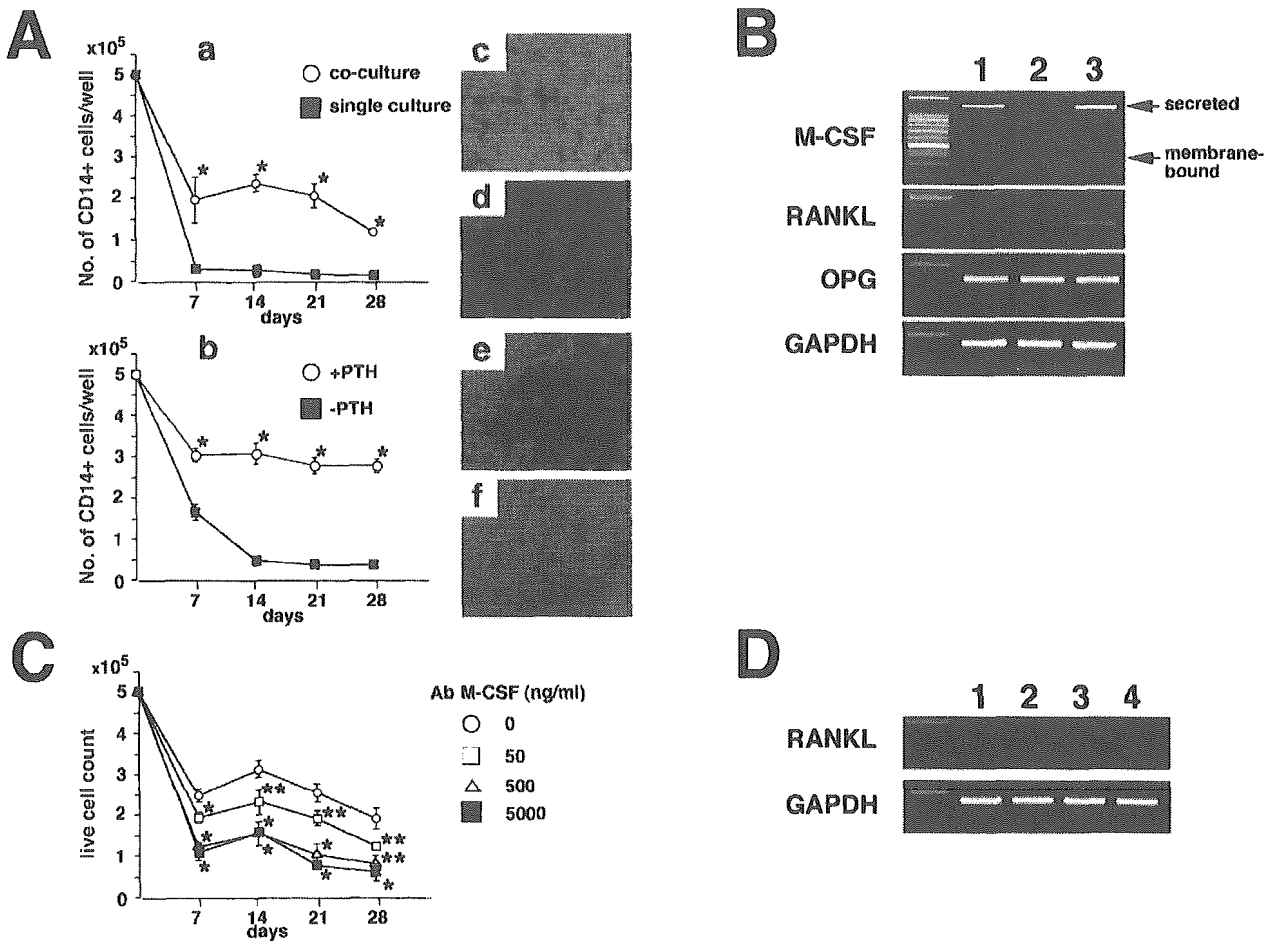

Figure 3. Importance of monocyte colony-stimulating factor (M-CSF) produced by SaOS-4/3 cells and nurse-like cells (NLCs) in the maintenance of CD14+ monocytes. **A**, Survival of CD14+ monocytes in cultures with or without NLCs or SaOS-4/3 cells. **a**, CD14+ monocytes were cultured with and without NLCs for 28 days, and the number of CD14+ monocytes recovered each week was counted. **b**, CD14+ monocytes were cultured with SaOS-4/3 cells in the presence and absence of parathyroid hormone (PTH; $10^{-8}M$), and the number of CD14+ monocytes recovered each week was counted. * = $P < 0.01$. **c** and **d**, Monocyte cultures with and without NLCs, respectively. **e** and **f**, Monocyte cultures with SaOS-4/3 cells in the presence and absence of PTH, respectively. (Original magnification × 40.) **B**, Total RNA was extracted from NLCs (lane 1) and from SaOS-4/3 cells treated for 3 days with (lane 2) or without (lane 3) PTH ($10^{-8}M$), and the expression of mRNA for M-CSF (secreted and membrane-bound forms), RANKL, osteoprotegerin (OPG), and GAPDH was analyzed by reverse transcription–polymerase chain reaction (RT-PCR). **C**, CD14+ monocytes were cocultured with NLCs in the presence of increasing concentrations of neutralizing antibodies (Ab) against human M-CSF, and the number of CD14+ monocytes recovered each week was counted. ★ = $P < 0.01$; ★★ = $P < 0.05$ versus cultures without antibodies. **D**, NLCs were treated with vehicle (control) (lane 1), PTH ($10^{-8}M$) (lane 2), prostaglandin E_2 ($10^{-6}M$) (lane 3), and 1α,25-dihydroxyvitamin D_3 ($10^{-8}M$) (lane 4). After 23 days, total RNA was extracted from NLCs, and the expression of mRNA for RANKL and GAPDH was analyzed by RT-PCR.

Osteoclast formation from CD14+ and NCD14+ monocytes in coculture with SaOS-4/3 cells. When NCD14+ monocytes were cocultured for 7 days with SaOS-4/3 cells, TRAP+ and VNR+ osteoclasts formed in the presence of PTH (Figure 2A). This osteoclast formation was completely inhibited by the addition of OPG. The mRNA for CTR, one of the most reliable signals for osteoclast differentiation, was detected in the coculture treated with PTH, but not in the coculture treated with PTH together with OPG (Figure 2B). Thus, NCD14+ monocytes differentiated into osteoclasts through their interaction with specialized stromal cells

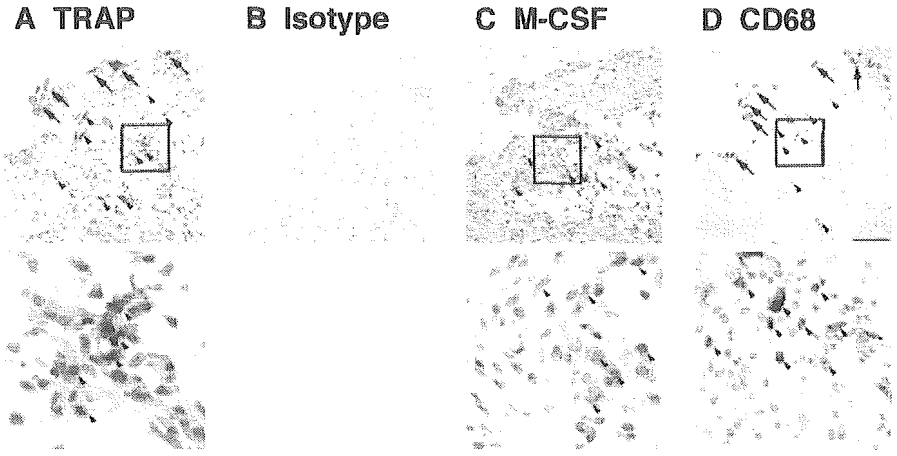

Figure 4. Localization of cells positive for tartrate-resistant acid phosphatase (TRAP), macrophage colony-stimulating factor (M-CSF), and CD68 in areas adjacent to the interface between bone and the progressive expansion of synovium in patients with rheumatoid arthritis. **A,** Some specimens stained positive for TRAP. **Arrows** indicate TRAP+ multinucleated cells; **arrowheads** indicate TRAP+ mononuclear cells. The other specimens were immunohistochemically stained with **B,** isotype control. **C,** antibodies against human M-CSF, and **D,** antibodies against CD68. **Arrowheads** in **C** indicate M-CSF+ synovial cells. **Arrowheads** in **D** indicate CD68+ monocytes; **arrows** in **D** indicate CD68+ multinucleated osteoclasts. Boxed areas in **A, C,** and **D** are shown at higher magnification underneath the respective panels (original magnification × 100). Bar = 100 μm.

that possess the ability to support osteoclast differentiation.

Involvement of M-CSF in the NLC-supported survival of CD14+ monocytes. When CD14+ monocytes were cultured without NLCs, almost all of the CD14+ monocytes disappeared within a week (Figure 3A, parts a and d). Approximately 40% of CD14+ monocytes survived for 4 weeks in coculture with NLCs (Figure 3A, parts a and c). SaOS-4/3 cells could not promote the survival of CD14+ monocytes in the absence of PTH (Figure 3A, parts b and f). However, treatment of the coculture with PTH enhanced the survival of CD14+ monocytes (Figure 3A, parts b and e). Furthermore, multinucleated cells were observed after a 4-week culture in the PTH-treated coculture (Figure 3A, part e). In contrast, multinucleated cells were not detected in cocultures with NLCs (Figure 3A, part c). These results suggested that PTH induced the expression of a cytokine(s) that promoted the survival of CD14+ monocytes and their resultant osteoclast formation.

We previously reported that treatment of SaOS-4/3 cells with PTH stimulated the expression of mRNA for both the membrane-associated and secreted forms of M-CSF (21). RT-PCR analysis showed that NLCs constitutively expressed mRNA for the secreted form of M-CSF and for OPG, but not for RANKL (Figure 3B). In contrast, neither M-CSF mRNA nor RANKL mRNA was expressed in SaOS-4/3 cells in the absence of PTH, but the expression of mRNA for both the membrane-associated and secreted forms of M-CSF as well as for RANKL was induced in PTH-treated SaOS-4/3 cells (Figure 3B). OPG mRNA expression in SaOS-4/3 cells was not affected by PTH.

When cocultures of CD14+ monocytes and NLCs were treated with neutralizing antibodies against human M-CSF, the number of CD14+ monocytes that survived in the coculture decreased in a dose-dependent manner (Figure 3C). Higher concentrations of the antibody (500 and 5,000 ng/ml) almost completely blocked the survival of CD14+ monocytes in the coculture. In contrast to SaOS-4/3 cells, NLCs failed to express RANKL mRNA in response to PTH, PGE_2, or $1\alpha,25(OH)_2D_3$, which are known to stimulate RANKL expression in mouse osteoblasts/bone marrow stromal cells (Figure 3D). Osteoclasts were not formed in the coculture of NLCs and CD14+ monocytes, even in the presence of such RANKL-inducing factors (data not shown).

Histologic examination of sites of bone destruction in RA patients. We examined the distribution of CD68+ monocytes, TRAP+ osteoclasts, and M-CSF+

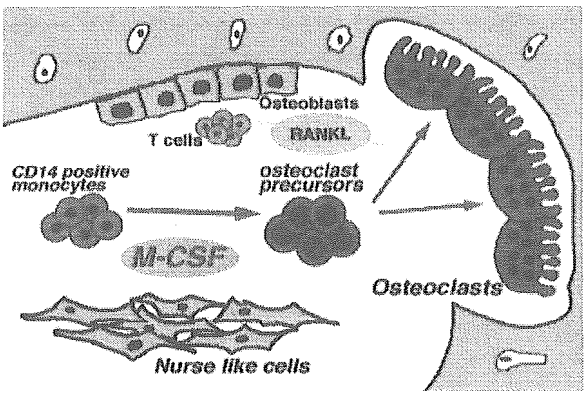

Figure 5. Possible role of nurse-like cells (NLCs) in bone destruction during progressive synovial expansion in rheumatoid arthritis (RA). NLCs show characteristics of fibroblast-like synoviocytes. NLCs support the survival of CD14+ monocytes as osteoclast precursors through the production of macrophage colony-stimulating factor (M-CSF). The resultant osteoclast precursors differentiate into osteoclasts that resorb bone in response to RANKL produced by osteoblasts and activated T cells. Thus, fibroblast-like synoviocytes present in RA synovium play important roles in RA-induced bone destruction by maintaining CD14+ monocytes that do not lose the capacity to differentiate into osteoclasts.

stromal cells in areas of progressive synovial expansion into bone in RA patients (Figure 4). TRAP+ multinucleated cells were detected along the surface of the bone and TRAP+ mononuclear cells were also detected in the pannus surrounding the damaged bone (Figure 4A). M-CSF+ cells were present in fibroblast-like synoviocytes surrounding areas of bone destruction (Figure 4C). CD68+ multinucleated cells and monocytes were detected at the bone–pannus interface and in the pannus surrounding the damaged bone (Figure 4D). Consistent with previous studies (12), we found that some multinucleated osteoclasts were positive for CD68. Thus, CD68+ monocytes and M-CSF+ synoviocytes were colocalized in areas adjacent to destroyed bone in RA patients.

DISCUSSION

In the present study, we demonstrated that NLCs support the survival of monocytes for a long period of time and that the resultant monocytes differentiate into osteoclasts in the presence of M-CSF together with RANKL or TNFα. Moreover, we revealed that M-CSF is one of the key molecules needed for NLCs to maintain monocytes without losing their capacity to differentiate into osteoclasts. CD68+ monocytes and M-CSF+ synoviocytes were colocalized in areas adjacent to destroyed bone in RA patients. These results suggest that fibroblast-like synoviocytes play an important role in bone destruction by continuously providing osteoclast precursors (Figure 5).

We compared the capacity of 2 types of cells, CD14+ and NCD14+ monocytes, to differentiate into osteoclasts. Consistent with the findings of previous studies (24–26), CD14+ monocytes differentiated into mature osteoclasts when stimulated with M-CSF and RANKL/TNFα. Mature osteoclasts were also generated from NCD14+ monocytes by treatment with M-CSF plus either RANKL or TNFα. NCD14+ monocytes expressed mRNA for RANK and TNFRI, suggesting that these cells could respond to RANKL and TNFα. SaOS-4/3 cells supported the differentiation of NCD14+ monocytes into osteoclasts in cocultures treated with PTH. Thus, NCD14+ monocytes interacted normally with stromal cells to receive RANKL and M-CSF signals. These results suggest that NCD14+ monocytes fulfill a phenotype of the osteoclast precursor.

M-CSF is known to induce the proliferation and maturation of monocyte/macrophages. SaOS-4/3 cells maintained CD14+ monocytes in the presence, but not the absence, of PTH. SaOS-4/3 cells produced M-CSF in response to PTH. NLCs constitutively expressed mRNA for the secreted type of M-CSF, and neutralizing antibodies against M-CSF strongly inhibited the NLC-supported survival of CD14+ monocytes. Using the mice transgenic for human TNFα as a model of erosive arthritis, Li et al (27) demonstrated that RANK signaling is not required for an increase in osteoclast precursors but is essential for osteoclast formation. Consistent with their finding, NLCs were able to support osteoclast precursors in the absence of RANKL. The monocyte-supporting activity found in NLCs appears to be a dominant trait of synovial cells. In fact, CD68+ monocytes and M-CSF+ synoviocytes were colocalized adjacent to areas of destroyed bone in RA patients. These results suggest that M-CSF produced by synoviocytes is involved not only in the formation of osteoclasts, but also in the maintenance of osteoclast precursors in the vicinity of RA-induced bone loss (Figure 5).

It is well known that M-CSF is synthesized by mesenchymal cells, including fibroblasts and osteoblasts (28–30). Therefore, we examined whether fibroblastic stromal cells other than SaOS-4/3 cells and NLCs could support the survival of CD14+ monocytes. Human skin fibroblasts derived from healthy volunteer donors and from human osteosarcoma MG63 cells supported the survival of CD14+ monocytes for 4 weeks, as the NLCs

had done (data not shown). These CD14+ monocytes obtained from cocultures with skin fibroblasts or MG63 cells differentiated into TRAP+ multinucleated cells in the presence of RANKL and M-CSF. These results support the conclusion that M-CSF produced by NLCs plays an essential role in the survival of osteoclast precursors for a long culture period.

The formation of osteoclasts from NCD14+ monocytes was observed in cocultures with SaOS-4/3 cells treated with PTH, but not those treated with NLCs. SaOS-4/3 cells expressed RANKL upon treatment with PTH, but NLCs could not express RANKL mRNA in response to any osteotropic factors. NLCs established from different patients all supported the survival of CD14+ monocytes (16), but none of them supported osteoclast formation in the presence of any osteotropic factors (data not shown). In contrast, several groups of researchers have reported that RA synovial fibroblasts support osteoclast formation in cocultures with peripheral blood mononuclear cells (11,26). Takayanagi et al (26) and Shigeyama et al (12) showed that RA synovial fibroblasts express RANKL in the presence of $1\alpha,25(OH)_2D_3$. Gravallese et al (10) reported that the expression of RANKL in synovial fibroblasts is difficult to detect in prolonged cultures. This assertion may support our findings concerning the characteristics of NLCs.

We previously demonstrated that NLCs may play an important role in disease pathogenesis by producing large amounts of cytokines and maintaining infiltrating lymphocytes (16,31). Burger et al (18,32) reported that blood-derived NLCs protect B cells from apoptosis through the production of stromal cell–derived factor 1. They also described the supporting mechanism, pseudoemperipolesis, in detail. Using Transwell culture plates, we confirmed that CD14+ monocytes survived for 4 weeks in the coculture with NLCs, even in the absence of the direct contact with NLCs. However, when those cells were further cultured with RANKL plus M-CSF, only a few osteoclasts were formed (data not shown). When cultured with M-CSF, CD14+ monocytes survived for 4 weeks, but could not differentiate into osteoclasts in the presence of M-CSF plus RANKL (data not shown). These results suggest that another unidentified stromal factor(s) is required to maintain CD14+ monocytes for a long period without the loss of their capacity to differentiate into osteoclasts.

Histologic examinations showed that numerous M-CSF+ stromal cells were detected in the vicinity of damaged bone in RA patients. Consistent with our results, it was previously shown that RA synovial fibroblasts expressed M-CSF (33) and that the concentration of M-CSF in synovial fluid was higher in RA patients than in patients with osteoarthritis (34). Moreover, a number of CD68+ cells and TRAP+ cells were colocalized in areas adjacent to the same sites of destroyed bone in RA patients. These results suggest that synoviocytes appear to participate in the recruitment and maintenance of osteoclast precursors in the vicinity of RA-induced bone loss (Figure 5).

In conclusion, our study suggests that NLCs are involved in RA-induced bone destruction by maintaining osteoclast precursors in areas of progressive synovial expansion. M-CSF constitutively produced by synovial fibroblasts is essential in the maintenance of osteoclast precursors in the vicinity of damaged bone. Therefore, blocking of the M-CSF pathway as well as the RANKL pathway may be a therapeutic target for the prevention of bone destruction caused by synovial expansion in patients with RA.

REFERENCES

1. Udagawa N, Takahashi N, Jimi E, Matsuzaki K, Tsurukai T, Itoh K, et al. Osteoblasts/stromal cells stimulate osteoclast activation through expression of osteoclast differentiation factor/RANKL but not macrophage colony-stimulating factor: receptor activator of NF-κB ligand. Bone 1999;25:517–23.
2. Suda T, Takahashi N, Udagawa N, Jimi E, Gillespie MT, Martin TJ. Modulation of osteoclast differentiation and function by the new members of the tumor necrosis factor receptor and ligand families. Endocr Rev 1999;20:345–57.
3. Teitelbaum SL. Bone resorption by osteoclasts. Science 2000;289: 1504–8.
4. Boyle WJ, Simonet WS, Lacey DL. Osteoclast differentiation and activation. Nature 2003;423:337–42.
5. Yasuda H, Shima N, Nakagawa N, Yamaguchi K, Kinosaki M, Mochizuki S, et al. Osteoclast differentiation factor is a ligand for osteoprotegerin/osteoclastogenesis-inhibitory factor and is identical to TRANCE/RANKL. Proc Natl Acad Sci U S A 1998;95: 3597–602.
6. Udagawa N, Takahashi N, Yasuda H, Mizuno A, Itoh K, Ueno Y, et al. Osteoprotegerin produced by osteoblasts is an important regulator in osteoclast development and function. Endocrinology 2000;141:3478–84.
7. Kobayashi K, Takahashi N, Jimi E, Udagawa N, Takami M, Kotake S, et al. Tumor necrosis factor α stimulates osteoclast differentiation by a mechanism independent of the ODF/RANKL-RANK interaction. J Exp Med 2000;191:275–86.
8. Jimi E, Nakamura I, Duong LT, Ikebe T, Takahashi N, Rodan GA, et al. Interleukin 1 induces multinucleation and bone-resorbing activity of osteoclasts in the absence of osteoblasts/stromal cells. Exp Cell Res 1999;247:84–93.
9. Tak PP, Bresnihan B. The pathogenesis and prevention of joint damage in rheumatoid arthritis: advances from synovial biopsy and tissue analysis. Arthritis Rheum 2000;43:2619–33.
10. Gravallese EM, Manning C, Tsay A, Naito A, Pan C, Amento E, et al. Synovial tissue in rheumatoid arthritis is a source of osteoclast differentiation factor. Arthritis Rheum 2000;43:250–8.
11. Takayanagi H, Iizuka H, Juji T, Nakagawa T, Yamamoto A, Miyazaki T, et al. Involvement of receptor activator of nuclear

factor κB ligand/osteoclast differentiation factor in osteoclastogenesis from synoviocytes in rheumatoid arthritis. Arthritis Rheum 2000;43:259–69.
12. Shigeyama Y, Pap T, Kunzler P, Simmen BR, Gay RE, Gay S. Expression of osteoclast differentiation factor in rheumatoid arthritis. Arthritis Rheum 2000;43:2523–30.
13. Hirayama T, Danks L, Sabokbar A, Athanasou NA. Osteoclast formation and activity in the pathogenesis of osteoporosis in rheumatoid arthritis. Rheumatology (Oxford) 2002;41:1232–9.
14. Wekerle H, Ketelsen UP. Thymic nurse cells: Ia-bearing epithelium involved in T-lymphocyte differentiation? Nature 1980;283: 402–4.
15. Iwagami S, Furue S, Toyosaki T, Horikawa T, Doi H, Satomi S, et al. Establishment and characterization of nurse cell-like clones from human skin: nurse cell-like clones can stimulate autologous mixed lymphocyte reaction. J Immunol 1994;153:2927–38.
16. Takeuchi E, Tomita T, Toyosaki-Maeda T, Kaneko M, Takano H, Hashimoto H, et al. Establishment and characterization of nurse cell–like stromal cell lines from synovial tissues of patients with rheumatoid arthritis. Arthritis Rheum 1999;42:221–8.
17. Tomita T, Takeuchi E, Toyosaki-Maeda T, Oku H, Kaneko M, Takano H, et al. Establishment of nurse-like stromal cells from bone marrow of patients with rheumatoid arthritis: indication of characteristic bone marrow microenvironment in patients with rheumatoid arthritis. Rheumatology (Oxford) 1999;38:854–63.
18. Burger JA, Zvaifler NJ, Tsukada N, Firestein GS, Kipps TJ. Fibroblast-like synoviocytes support B-cell pseudoemperipolesis via a stromal cell-derived factor-1- and CD106 (VCAM-1)-dependent mechanism. J Clin Invest 2001;107:305–15.
19. Toyosaki-Maeda T, Takano H, Tomita T, Tsuruta Y, Maeda-Tanimura M, Shimaoka Y, et al. Differentiation of monocytes into multinucleated giant bone-resorbing cells: two-step differentiation induced by nurse-like cells and cytokines. Arthritis Res 2001;3: 306–10.
20. Matsuzaki K, Katayama K, Takahashi Y, Nakamura I, Udagawa N, Tsurukai T, et al. Human osteoclast-like cells are formed from peripheral blood mononuclear cells in a coculture with SaOS-2 cells transfected with the parathyroid hormone (PTH)/PTH-related protein receptor gene. Endocrinology 1999;140:925–32.
21. Itoh K, Udagawa N, Matsuzaki K, Takami M, Amano H, Shinki T, et al. Importance of membrane- or matrix-associated forms of M-CSF and RANKL/ODF in osteoclastogenesis supported by SaOS-4/3 cells expressing recombinant PTH/PTHrP receptors. J Bone Miner Res 2000;15:1766–75.
22. Arnett FC, Edworthy SM, Bloch DA, McShane DJ, Fries JF, Cooper NS, et al. The American Rheumatism Association 1987 revised criteria for the classification of rheumatoid arthritis. Arthritis Rheum 1988;31:315–24.
23. Kaneko M, Tomita T, Nakase T, Takeuchi E, Iwasaki M, Sugamoto K, et al. Rapid decalcification using microwaves for in situ hybridization in skeletal tissues. Biotech Histochem 1999;74: 49–54.
24. Nicholson GC, Malakellis M, Collier FM, Cameron PU, Holloway WR, Gough TJ, et al. Induction of osteoclasts from CD14-positive human peripheral blood mononuclear cells by receptor activator of nuclear factor κB ligand (RANKL). Clin Sci (Lond) 2000;99: 133–40.
25. Kudo O, Fujikawa Y, Itonaga I, Sabokbar A, Torisu T, Athanasou NA. Proinflammatory cytokine (TNFα/IL-1α) induction of human osteoclast formation. J Pathol 2002;198:220–7.
26. Takayanagi H, Oda H, Yamamoto S, Kawaguchi H, Tanaka S, Nishikawa T, et al. A new mechanism of bone destruction in rheumatoid arthritis: synovial fibroblasts induce osteoclastogenesis. Biochem Biophys Res Commun 1997;240:279–86.
27. Li P, Schwarz EM, O'Keefe RG, Ma L, Boyce BF, Xing L. RANK signaling is not required for TNFα-mediated induced in $CD11b^{high}$ osteoclast precursors but is essential for mature osteoclast formation in TNFα-mediated inflammatory arthritis. J Bone Miner Res 2004;19:207–13.
28. Yoshida H, Hayashi S, Kunisada T, Ogawa M, Nishikawa S, Okamura H, et al. The murine mutation osteopetrosis is in the coding region of the macrophage colony stimulating factor gene. Nature 1990;345:442–4.
29. Rettenmier CW, Roussel MF, Sherr CJ. The colony-stimulating factor 1 (CSF-1) receptor (c-fms proto-oncogene product) and its ligand. J Cell Sci Suppl 1988;9:27–44.
30. Stanley ER, Berg KL, Einstein DB, Lee PS, Pixley FJ, Wang Y, et al. Biology and action of colony-stimulating factor-1. Mol Reprod Dev 1997;46:4–10.
31. Shimaoka Y, Attrep JF, Hirano T, Ishihara K, Suzuki R, Toyosaki T, et al. Nurse-like cells from bone marrow and synovium of patients with rheumatoid arthritis promote survival and enhance function of human B cells. J Clin Invest 1998;102:606–18.
32. Burger JA, Tsukada N, Burger M, Zvaifler NJ, Dell'Aquila M, Kipps TJ. Blood-derived nurse-like cells protect chronic lymphocytic leukemia B cells from spontaneous apoptosis through stromal cell-derived factor-1. Blood 2000;96:2655–63.
33. Yamamoto M, Yasuda M, Shiokawa S, Nobunaga M. Effects of colony-stimulating factors on proliferation and activation of synovial cells. Clin Rheumatol 1991;10:277–82.
34. Kawaji H, Yokomura K, Kikuchi K, Somoto Y, Shirai Y. Macrophage colony-stimulating factor in patients with rheumatoid arthritis. Nippon Ika Daigaku Zasshi 1995;62:260–70.

J Artif Organs (2005) 8:131–136
DOI 10.1007/s10047-005-0292-1

REVIEW

Hideki Yoshikawa, MD, PhD · Akira Myoui, MD, PhD

Bone tissue engineering with porous hydroxyapatite ceramics

Abstract The main principle of bone tissue engineering strategy is to use an osteoconductive porous scaffold in combination with osteoinductive molecules or osteogenic cells. The requirements for a scaffold in bone regeneration are: (1) biocompatibility, (2) osteoconductivity, (3) interconnected porous structure, (4) appropriate mechanical strength, and (5) biodegradability. We recently developed a fully interconnected porous hydroxyapatite (IP-CHA) by adopting the "form-gel" technique. IP-CHA has a three-dimensional structure with spherical pores of uniform size that are interconnected by window-like holes; the material also demonstrated adequate compression strength. In animal experiments, IP-CHA showed superior osteoconduction, with the majority of pores filled with newly formed bone. The interconnected porous structure facilitates bone tissue engineering by allowing the introduction of bone cells, osteotropic agents, or vasculature into the pores. In this article, we review the accumulated data on bone tissue engineering using the novel scaffold, focusing especially on new techniques in combination with bone morphogenetic protein (BMP) or mesenchymal stem cells.

Key words Bone · Hydroxyapatite ceramics · Tissue engineering · Mesenchymal cell

Introduction

Bone tissue has a vigorous potential for regeneration in itself, as observed in fracture healing. However, to reconstruct a large bony defect or to treat poor bone-healing conditions, bone grafts are required. Up to the present, autogenous bone grafting has been the gold standard because of its obvious advantages in osteogenic capacity, osteoconduction, mechanical properties, and the lack of adverse immunological response. On the other hand, autogenous bone grafting techniques have some limitations,[1] such as the requirement of additional surgery for harvesting, the availability of grafts of sufficient size and shape, and the risk of donor site morbidity,[2–4] which may include fracture, long-lasting pain, nerve damage, and infection. Therefore, in the field of orthopedics or craniofacial surgery, many kinds of biomaterials have been developed as bone substitutes, such as ceramics, polymers, metals, and organic or non-organic bone substitutes.[5–9]

Among them, hydroxyapatite (HA) ceramics have been used extensively as a substitute in bone grafts,[10–14] because the crystalline phase of natural bone is basically HA. The ceramics are available as dense or porous types and as granules or blocks. Different pore sizes, porosities, and strengths are also available. However, recent clinical evidence has revealed that the pores are not replaced with new bone for a substantial period of time, probably due to the limited interconnection of the pores.[15] We recently developed a fully interconnected porous form of hydroxyapatite ceramic (IP-CHA) to overcome this disadvantage.[16] Another problem of HA is that it is osteoconductive, but not osteoinductive. If the ceramics themselves possessed bone-forming activity, their clinical applications would be greatly expanded. With these facts in mind, we have tried to develop a new bone tissue engineering system using IP-CHA in combination with bone morphogenetic protein (BMP), mesenchymal stem cells from bone marrow, and vascular prefabrication.

Received: February 4, 2005

H. Yoshikawa (✉) · A. Myoui
Department of Orthopaedics, Osaka University Graduate School of Medicine, 2-2 Yamadaoka, Suita 565-0871, Japan
Tel. +81-6-6879-3550; Fax +81-6-6879-3559
e-mail: yhideki@ort.med.osaka-u.ac.jp

Interconnected porous hydroxyapatite ceramics

We have developed a fully interconnected porous HA ceramic (IP-CHA, NEOBONE): porosity 75%, average pore size 150μm, and average interpore connections 40μm, by adopting the "foam-gel" technique (Fig. 1).[16] This approach

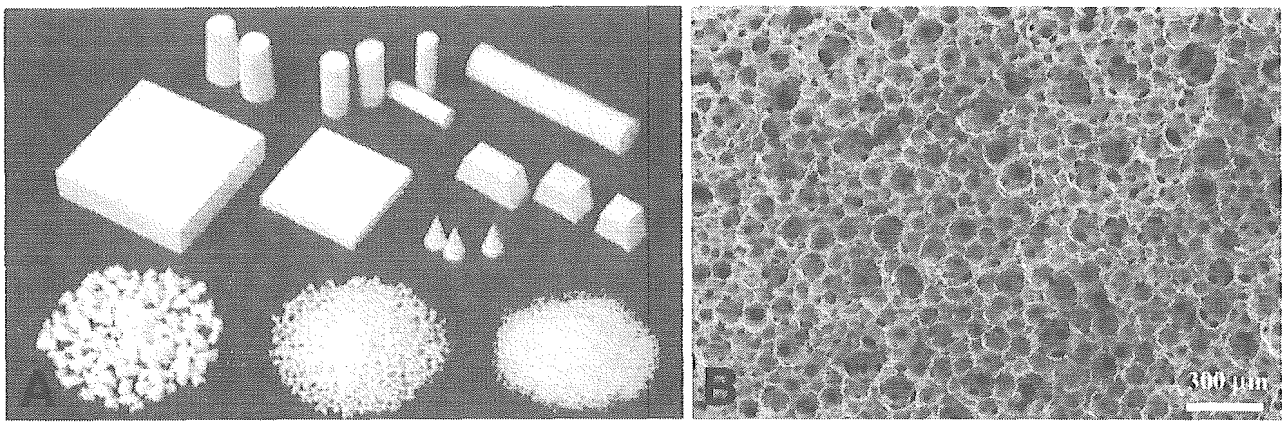

Fig. 1A,B. Macroscopic and microscopic photographs of interconnected porous hydroxyapatite (IP-CHA, NEOBONE). **A** The different types of IP-CHA. The materials were manufactured by Toshiba Ceramics. **B** Scanning electron microscopy (SEM) showed the microstructures of IP-CHA. Spherical pores (100–200μm in diameter) were divided by thin walls and interconnected by interpores (10–80μm in diameter)

involves a crosslinking polymerization step that gelatinizes the foam-like CHA slurry in a rapid manner, thus promoting the formation of an interconnected porous structure. The wall surface of IP-CHA is very smooth and HA particles are aligned closely to one another and bound tightly.

In IP-CHA, the majority of the interpore connections ranged from 10–80μm in diameter, with a maximum peak at about 40μm, which would theoretically be permissive to cell migration or tissue invasion from pore to pore.[17] The compression strength of IP-CHA is 12MPa, while the compression strength of cancellous bone is 1–12MPa.[18]

Osteoconduction in vivo

We histologically analyzed bone ingrowth in cylindrical blocks (6mm in diameter) of IP-CHA using the rabbit femoral condyle model.[16,19] Within 6 weeks after implantation of IP-CHA, mature bone ingrowth was seen in all the pores throughout the block. In the pores, bone, bone marrow formation through interpore connections with osteoblastic rimming, and vessels were all observed. We also examined the sequential change in the compression strength of the IP-CHA implanted in rabbit femoral condyle. The initial compressive strength of IP-CHA was approximately 10–12MPa. The implanted IP-CHA steadily increased its compressive strength with time until 9 weeks after implantation, finally reaching a value of about 30MPa.[16,19]

Bone tissue engineering with bone morphogenetic protein

Bone morphogenetic protein (BMP) is a biologically active molecule capable of inducing new bone formation.[20,21] We have analyzed the efficacy of IP-CHA as a delivery system for recombinant human BMP-2 (rhBMP-2). We combined two biomaterials to construct a carrier/scaffold system for rhBMP-2: IP-CHA and a synthetic biodegradable polymer poly D,L-lactic acid–polyethyleneglycol block co-polymer (PLA-PEG).[22,23] We used a rabbit radius model to evaluate the bone-regenerating activity of rhBMP-2/PLA-PEG/IP-CHA composite. At 8 weeks after implantation, all bone defects in groups treated with 5μg of rhBMP-2 were completely repaired with sufficient strength (Fig. 2).[24] Using this carrier scaffold system, we reduced the amount of rhBMP-2 necessary for such results to about a tenth of the amount needed in previous studies. Enhancement of bone formation is probably due to the superior osteoconduction ability of IP-CHA and the optimal drug delivery system provided by PLA-PEG. The synthetic biodegradable polymer PLA-PEG/IP-CHA composite is an excellent carrier/scaffold delivery system for rhBMP-2, and strongly encourages the clinical effects of rhBMP-2 in bone tissue regeneration.

Bone tissue engineering with mesenchymal stem cells

We investigated whether IP-CHA can be utilized as a scaffold for cell-based bone tissue engineering using the rat subcutaneous model of Ohgushi et al.[25,26] We used bone-derived mesenchymal stem cells as a source of bone-producing cells. Bone marrow cells were collected from the femur of rats and were cultivated in minimal essential medium supplemented with 15% fetal bovine serum. IP-CHA discs ($R = 5$mm, $h = 2$mm) were soaked in the cell suspension overnight and further cultured in the same medium with β-glycerophosphate, ascorbic acid, and dexamethasone for 14 days. The discs were then implanted into the subcutaneous tissue of rats and harvested 2–8 weeks after implantation. All the implants showed bone formation inside the pore areas as evidenced by decalcified histological sections and microcomputed tomography images (Fig. 3).[27,28] The

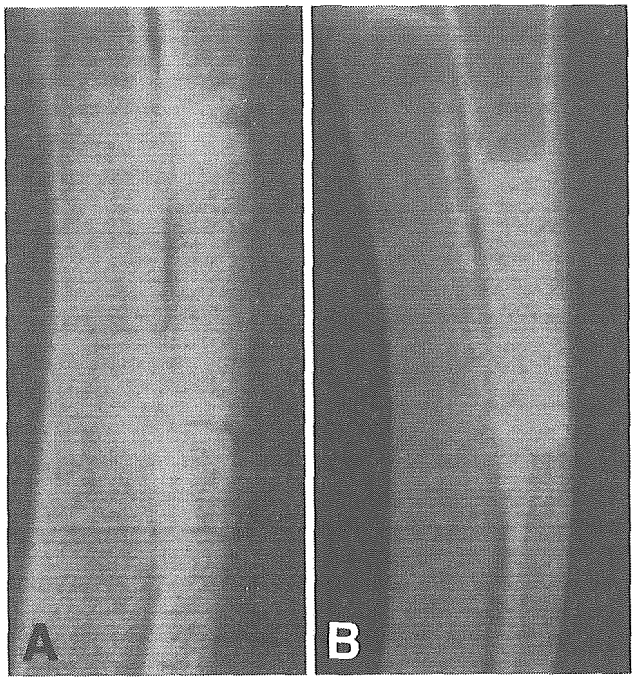

Fig. 2A,B. Soft X-ray photographs of the healing of a bone defect in a rabbit radius. **A** The IP-CHA-alone group at 8 weeks after implantation. *Radiolucent lines* are clearly visible between the IP-CHA and host bone, and the radiodensity of IP-CHA did not increase. **B** The recombinant human bone morphogenetic protein 2 (rhBMP-2, 5 μg)/IP-CHA group at 8 weeks after implantation. Bony unions were observed at the junction sites and the radiodensity of IP-CHA increased

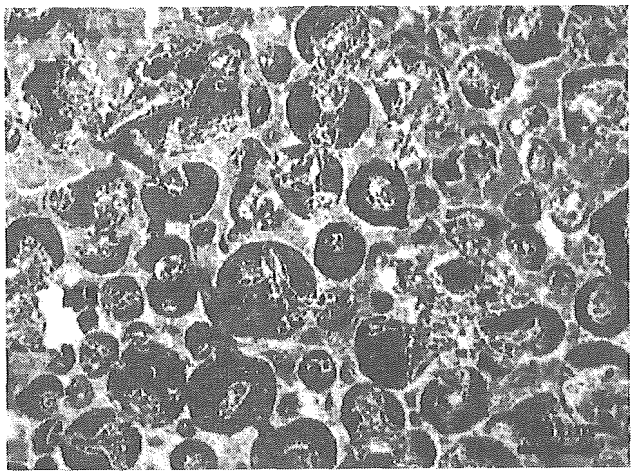

Fig. 3. New bone formation within the IP-CHA with bone marrow-derived mesenchymal stem cells. The IP-CHA was recovered from rat subcutaneous tissue 4 weeks after implantation. Most of the pores were filled with newly formed bone (H.E. staining)

bone volume increased over time. At 8 weeks after implantation, extensive bone volume was detected not only in the surface pore areas but also in the center pore areas of the implants. The combination of IP-CHA and mesenchymal cells could be used as an excellent bone graft substitute because of its mechanical properties and capability of inducing bone formation.

Bone tissue engineering with vascular prefabrication

A vascular network and sufficient blood supply are essential for bone regeneration. Introduction of vasculature into porous implants is another important aspect in regeneration for larger bone defects. We investigated the possibility of integrating IP-CHA with a capillary vessel network via insertion of a vascular pedicle to determine whether this procedure enhanced new bone formation in tissue engineering. This kind of approach to support blood supply generation in porous biomaterials has also been reported by others using subcutaneous tissue and muscle flaps.[29,30] IP-CHA loaded with 10 μg of rhBMP-2 was implanted subcutaneously into rat groin with insertion of superficial inferior epigastric vessels. At 3 weeks, IP-CHA/BMP composite with vascular insertion exhibited abundant new bone formation in the pores of the deep portion close to the inserted vessels (Fig. 4).[19,31] This novel system of integrating a vascular network with IP-CHA is considered a useful technique for bone tissue engineering.

Application for cartilage repair

Several investigators have reported on the repair of articular cartilage defects using diverse approaches such as gene-enhanced techniques, direct injection of growth factors, and in vitro cell expansion,[32-34] but the repair remains a major obstacle in tissue engineering. We developed a new technology for articular cartilage repair, consisting of a triple composite of rhBMP-2, PLA-PEG polymer and IP-CHA, to induce regeneration of both subchondral bone and articular cartilage. Full-thickness cartilage defects in the rabbit were filled with the rhBMP-2 (20 μg)/PLA-PEG/IP-CHA composite. One week after implantation, a vigorous repair had occurred in the subchondral defect and an agglomeration of mesenchymal cells, migrated from the surrounded bone marrow via the interconnecting pores of the IP-CHA, was detected. At 6 weeks, subchondral defects were completely repaired by subchondral bone and articular cartilage covered the bone (Fig. 5).[35] The regenerated cartilage manifested a hyaline-like appearance, with a columnar organization of chondrocytes and a mature matrix. This novel cell-free technology using the triple composite of rhBMP-2, PLA-PEG, and IP-CHA could mark a new development in the field of articular cartilage repair.

Conclusion and perspectives

The three-dimensional fully interconnected porous structure of IP-CHA encourages bone ingrowth in the material

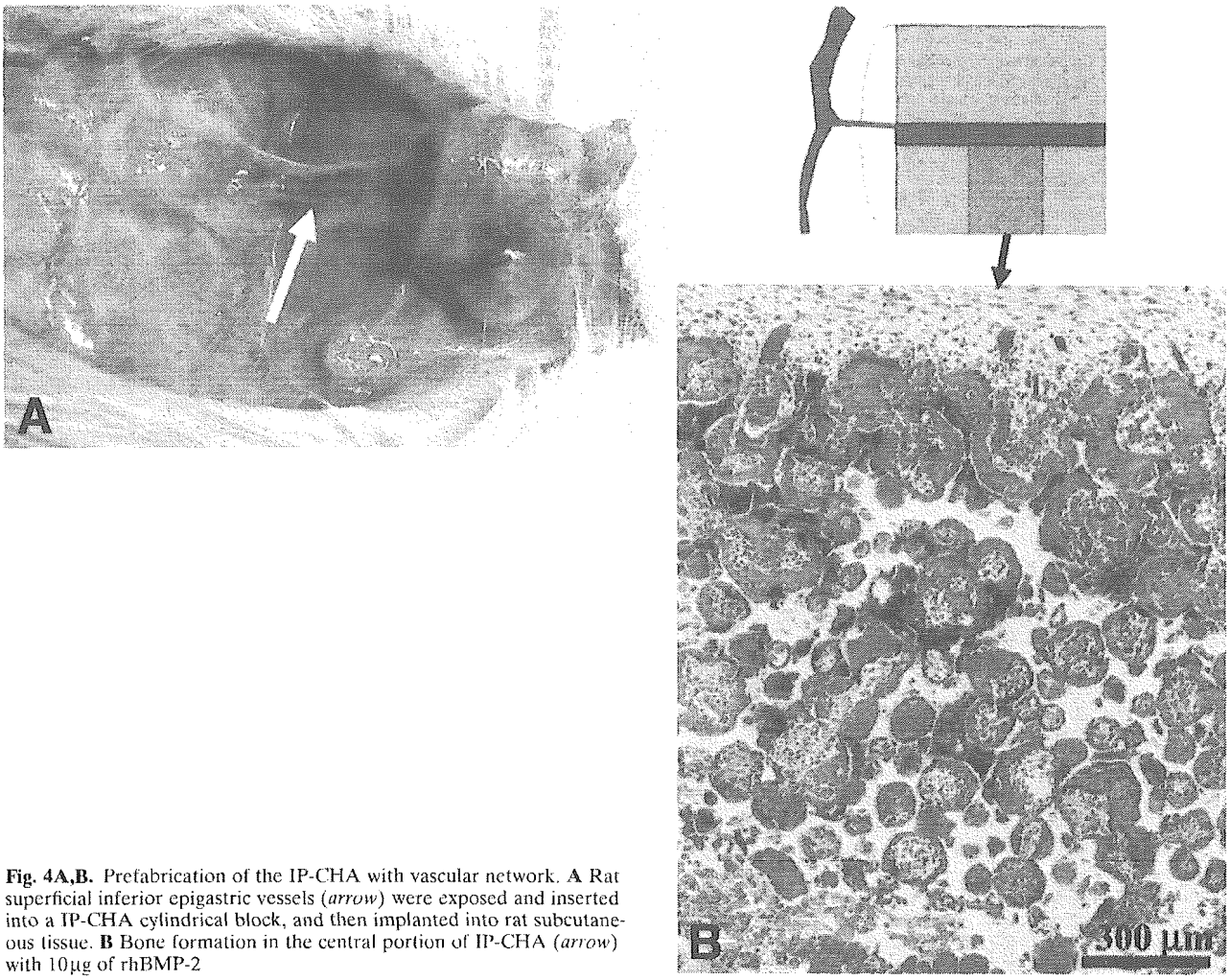

Fig. 4A,B. Prefabrication of the IP-CHA with vascular network. **A** Rat superficial inferior epigastric vessels (*arrow*) were exposed and inserted into a IP-CHA cylindrical block, and then implanted into rat subcutaneous tissue. **B** Bone formation in the central portion of IP-CHA (*arrow*) with 10μg of rhBMP-2

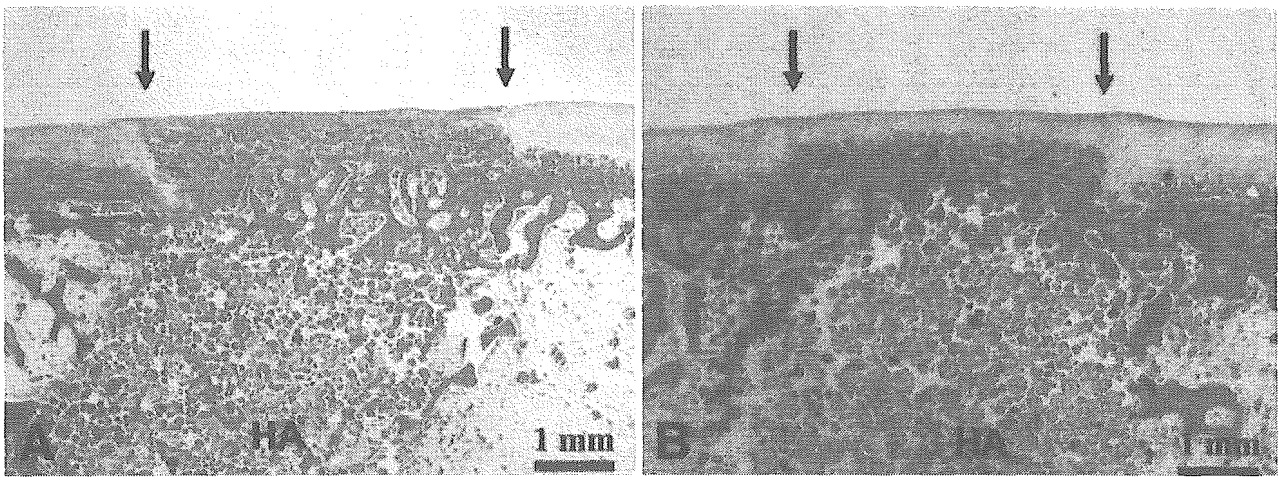

Fig. 5A,B. Articular cartilage repair by the BMP/poly D,L,-lactic acid–polyethylenglycol (PLA-PEG)/IP-CHA composite. *Arrows* indicate the margins of the defect: *HA*, IP-CHA (H.E. staining). **A** PLA-PEG/IP-CHA group at 6 weeks after implantation. Subchondral bone was regenerated, but no articular cartilage was observed. **B** BMP/PLA-PEG/IP-CHA group at 6 weeks after implantation. Well-organized hyaline-like cartilage covering the regenerated subchondral bone was observed

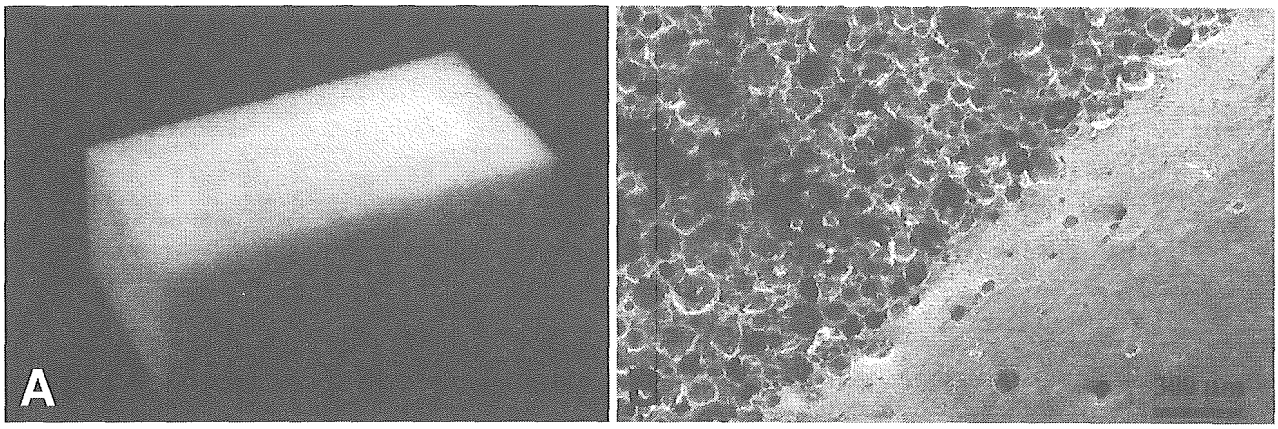

Fig. 6. Macroscopic (**A**) and microscopic (SEM) (**B**) photographs of the solid/interconnected porous HA composite

and eventually leads to good incorporation of the material into host bone. The synthetic scaffold can be prefabricated into specific sizes and shapes to match bone defects, and even into a composite with the solid form of HA in order to reinforce its initial mechanical strength (Fig. 6). We believe that IP-CHA itself is an excellent bone substitute for filling bone defects and should be considered as an alternative to autogenous bone. In addition, IP-CHA could serve as a good scaffold for cytokine-based or cell-based tissue-engineered bone and cartilage. In fact, we have been successful in bone tissue engineering using rhBMP-2, mesenchymal cells, or vasculature in animals. IP-CHA can be also applied to articular cartilage repair. IP-CHA is now commercially available, and we have applied IP-CHA as a bone substitute for the treatment of more than 50 patients with benign bone tumors or nonunion of a fracture, and obtained some favorable clinical results. Recently, we started a clinical study with the combination of IP-CHA and autologous mesenchymal cells for bone tissue repair. Additional studies with larger animals including dogs or monkeys and precise clinical evaluation are necessary, but we believe that bone tissue engineering with IP-CHA offers new approaches to the treatment of patients requiring skeletal reconstruction.

Acknowledgments The authors would like to thank Dr. Hajime Ohgushi for invaluable advice regarding bone tissue engineering using bone marrow cells, and Dr. Kunio Takaoka for invaluable advice regarding bone tissue engineering using rhBMP-2. We also thank Toshiba Ceramics Co., Ltd. and MMT Co., Ltd. for supplying materials. This work was supported in part by grants from the New Energy and Industrial Technology Development Organization (NEDO), the Ministry of Health, Labor and Welfare (OPSR), Japan, and the Ministry of Education, Culture, Sports, Science and Technology of Japan.

References

1. Prolo DJ, Rodrigo JJ. Contemporary bone graft physiology and surgery. Clin Orthop 1985;200:322–342
2. Arrington ED, Smith WJ, Chambers HG, Bucknell AL, Davino NA. Complications of iliac crest bone graft harvesting. Clin Orthop 1996;329:300–309
3. Banwart JC, Asher MA, Hassanein RS. Iliac crest bone graft harvest donor site morbidity. A statistical evaluation. Spine 1995;20: 1055–1060
4. Younger EM, Chapman MW. Morbidity at bone graft donor sites. J Orthop Trauma 1989;3:192–195
5. Bucholz RW, Carlton A, Holmes RE. Hydroxyapatite and tricalcium phosphate bone graft substitute. Orthop Clin North Am 1987;18:323–334
6. Ishihara K, Arai H, Nakabayashi N, Morita S, Furuya, KI. Adhesive bone cement containing hydroxyapatite particles as bone compatible filter. J Biomed Mater Res 1992;26:937–945
7. Sartoris DJ, Gershuni DH, Akeson WH, Holmes RE, Resnick D. Coralline hydroxyapatite bone graft substitutes: preliminary report of radiographic evaluation. Radiology 1986;159:133–137
8. Fujibayashi S, Kim HM, Neo M, Uchida M, Kokubo T, Nakamura T. Repair of segmental long bone defect in rabbit femur using bioactive titanium cylindrical mesh cage. Biomaterials 2003;24: 3445–3451
9. Cornell CN, Lane JM, Chapman M, Merkow R, Seligson D, Henry S, Gustilo R, Vincent K. Multicenter trial of Collagraft as bone graft substitute. J Orthop Trauma 1991;5:1–8
10. Holmes RE, Bucholz RW, Mooney V. Porous hydroxyapatite as a bone graft substitute in diaphyseal defects: a histometric study. J Orthop Res 1987;5:114–121
11. Bucholz RW, Carlton A, Holmes R. Interporous hydroxyapatite as a bone graft substitute in tibial plateau fractures. Clin Orthop 1989;240:53–62
12. Uchida A, Araki N, Shinto Y, Yoshikawa H, Kurisaki E, Ono K. The use of calcium hydroxyapatite ceramic in bone tumour surgery. J Bone Joint Surg 1990;72B:298–302
13. Yoshikawa H, Uchida A. Clinical application of calcium hydroxylapatite ceramic in bone tumor surgery. In: Wise DL (ed), Biomaterials and Bioengineering Handbook. New York: Marcel Dekker, 1999;433–455
14. Matsumine A, Myoui A, Kusuzaki K, Araki N, Seto M, Yoshikawa H, Uchida A. Calcium hydroxyapatite ceramic implants in bone tumor surgery. A long-term follow-up study. J Bone Joint Surg 2004;86B:719–725
15. Ayers RA, Simske SJ, Nunes CR, Wolford LM. Long-term bone ingrowth and residual micro hardness of porous block hydroxyapatite implants in humans. J Oral Maxillofac Surg 1998;56:1297–1301
16. Tamai N, Myoui A, Tomita T, Nakase T, Tanaka J, Ochi T, Yoshikawa H. Novel hydroxyapatite ceramics with an interconnective porous structure exhibit superior osteoconduction in vivo. J Biomed Mater Res 2002;59:110–117
17. Steinkamp JA, Hansen KM, Crissman HA. Flow microfluorometric and light-scatter measurement of nuclear and cytoplasmic size in mammalian cells. J Histochem Cytochem 1976; 24:292–297
18. Martin RB, Chapman MW, Sharkey NA, Zissimos SL, Bay B, Shors EC. Bone ingrowth and mechanical properties of coralline

hydroxyapatite 1 year after implantation. Biomaterials 1993;14: 341–348
19. Myoui A, Tamai N, Nishikawa M, Araki N, Nakase T, Akita S, Yoshikawa H. Three-dimensionally engineered hydroxyapatite ceramics with interconnected pores as a bone substitute and tissue engineering scaffold. In: Yaszemski MJ, Trantolo DJ, Lewandrowski KU, Hasirci V, Altobelli DE, Wise DL (eds) Biomaterials in orthopedics. New York: Marcel Dekker, 2004;287–300
20. Urist MR. Bone: formation by autoinduction. Science 1965;150: 893–899
21. Wozney JM, Rosen V. Bone morphogenetic protein and bone morphogenetic protein gene family in bone formation and repair. Clin Orthop 1998;346:26–37
22. Miyamoto S, Takaoka K, Okada T, Yoshikawa H, Hashimoto J, Suzuki S, Ono K. Polylactic acid–polyethylene glycol block copolymer: a new biodegradable synthetic carrier for bone morphogenetic protein. Clin Orthop 1993;294:333–343
23. Saito N, Okada T, Horiuchi H, Murakami N, Takahashi J, Nawata M, Ota H, Miyamoto S, Nozaki K, Takaoka K. Biodegradable polylactic acid–polyethylene glycol block copolymers as a BMP delivery system for inducing bone. J Bone Joint Surg 2001;83A:S92–S98
24. Kaito T, Myoui A, Takaoka K, Saito N, Nishikawa M, Tamai N, Ohgushi H, Yoshikawa H. Potentiation of the activity of bone morphogenetic protein-2 in bone regeneration by a PLA-PEG/hydroxyapatite composite. Biomaterials 2005;26:73–79
25. Ohgushi H, Caplan AI. Stem cell technology and bioceramics: from cell to gene engineering. J Biomed Mater Res 1999;48:913–927
26. Ohgushi H, Dohi Y, Katuda T, Tamai S, Tabata S, Suwa Y. In vitro bone formation by rat marrow cell culture. J Biomed Mater Res 1996;32:333–340
27. Nishikawa M, Myoui A, Ohgushi H, Ikeuchi M, Tamai N, Yoshikawa H. Bone tissue engineering using novel interconnected porous hydroxyapatite ceramics combined with marrow mesenchymal cells: Quantitative and three-dimensional image analysis. Cell Transplant 2004;13:367–376
28. Nishikawa M, Ohgushi H. Calcium phosphate ceramics in Japan. In: Yaszemski MJ, Trantolo DJ, Lewandrowski KU, Hasirci V, Altobelli DE, Wise DL (eds) Biomaterials in orthopedics. New York: Marcel Dekker, 2004;425–436
29. Bernard SL, Picha GJ. The use of coralline hydroxyapatite in a "biocomposite" free flap. Plast Reconstr Surg 1991;87:96–105
30. Casabona F, Martin I, Muraglia A, Berrino P, Santi P, Cancedda R, Quarto R. Prefabricated engineered bone flaps: an experimental model of tissue reconstruction in plastic surgery. Plast Reconstr Surg 1998;101:577–581
31. Akita S, Tamai N, Myoui A, Nishikawa M, Kaito T, Takaoka K, Yoshikawa H. Capillary vessel network integration by inserting a vascular pedicle enhances bone formation in tissue-engineered bone using interconnected porous hydroxyapatite ceramics. Tissue Eng 2004;10:789–795
32. Wakitani S, Imoto K, Yamamoto T, Saito M, Murata N, Yoneda M. Human autologous culture expanded bone marrow mesenchymal cell transplantation for repair of cartilage defects in osteoarthritic knees. Osteoarthritis Cartilage 2002;10:199–206
33. Cook SD, Patron LP, Salkeld SL, Rueger DC. Repair of articular cartilage defects with osteogenic protein-1 (BMP-7) in dogs. J Bone Joint Surg 2003;85A:116–123
34. Hidaka C, Goodrich LR, Chen CT, Warren RF, Crysta RG, Nixon AJ. Acceleration of cartilage repair by genetically modified chondrocyte overexpressing bone morphogenetic protein-7. J Orthop Res 2003;21:573–583
35. Tamai N, Myoui A, Hirao M, Kaito T, Ochi T, Tanaka J, Takaoka K, Yoshikawa H. A new biotechnology for articular cartilage repair: subchondral implantation of a composite of interconnected porous hydroxyapatite, synthetic polymer (PLA/PEG), and bone morphogenetic protein-2 (rhBMP-2). Osteoarthritis Cartilage, 2005;13:405–417

連通多孔体ハイドロキシアパタイトと骨髄間葉系細胞を用いた骨再生*

西川昌孝
名井　陽
大串　始
池内正子
玉井宣行
吉川秀樹**

[別冊整形外科 47：7～11，2005]

はじめに

整形外科分野において骨腫瘍，外傷，リウマチ性疾患，人工関節置換術後の弛みなどに対し，骨盤や腓骨などからの自家骨移植が行われてきた．しかし，採骨に伴う手術侵襲，採骨部の術後骨折などの合併症や採骨量の限界などの問題がある．今日までこれらの問題を解決するためアルミナ，バイオグラス，ハイドロキシアパタイト（HA）などさまざまな素材が使用されてきた．HA は生体適合性と骨伝導能を有した骨補塡材料であるが，近年まで用いられてきた合成多孔体 HA には十分な連通多孔体構造が存在していない．連通多孔体 HA［NEOBONE®：東芝セラミックス社，東京］は平均気孔径 150 μm，平均連通孔径 40 μm，気孔率 75%であるが，その連通構造のため深部気孔内にまで細胞が進入することができ，従来の多孔体 HA に比べ優れた骨伝導能を示す[1]．しかし，このように優れた骨伝導能をもつ NEOBONE® でさえ骨誘導能はもたず，巨大な欠損や感染後などの劣悪な骨再生環境では人工骨単体では十分な骨再生を得られない．

近年，再生組織工学の手法を用いた新鮮骨髄細胞や培養増殖させた骨髄間葉系細胞（marrow mesenchymal cells：MMCs）を導入した多孔体 HA の骨形成能が報告されており[2～9]，連通多孔体構造をもつ NEOBONE® は骨形成細胞を容易に気孔内に導入することができる．今回骨再生組織工学の担体としての NEOBONE® の有用性を検討した．

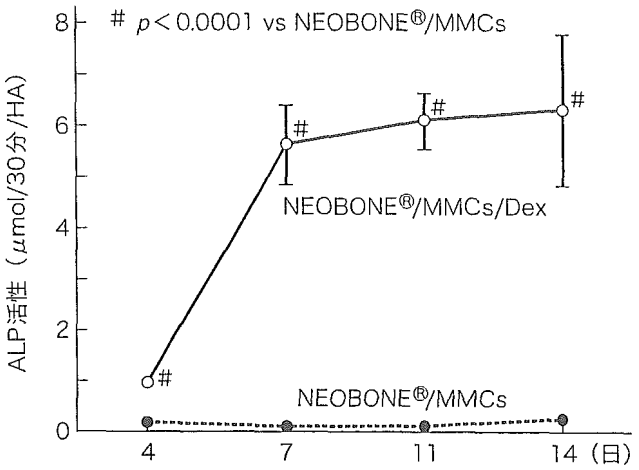

図1．NEOBONE® 培養人工骨の *in vitro* でのアルカリホスファターゼ（ALP）活性．デキサメタゾン（Dex）の添加培養により骨芽細胞への初期分化マーカーである ALP 活性は 7 日目から高値を示した．

Ⅰ．培養人工骨の作成

Fischer 344 ラットの大腿骨から採取した骨髄細胞を培養し，MMCs を回収した[10]．これを Yoshikawa ら[11]の方法に準じて 10^6細胞/ml の細胞浮遊液に調整し，直径 5 mm，厚さ 2 mm の円盤状に形成した NEOBONE® ならびにほかの 3 つの日本の合成多孔体 HA（HA-A，HA-B，HA-C）を一晩浸し，細胞を接着させた．次にデキサメタゾン（Dex），β-グリセロリン酸，ビタミン C 存在下で培養分化させたのち，同系ラットの皮下に移植した．

Key words
bone tissue engineering，hydroxyapatite，marrow mesenchymal cell

*Bone tissue engineering using interconnected porous calcium hydroxyapatite loaded marrow mesenchymal cells
要旨は第 25 回日本バイオマテリアル学会において発表した．

**M. Nishikawa，A. Myoui：大阪大学大学院医学系研究科器官制御外科学整形外科（Dept. of Orthop，Osaka University Graduate School of Medicine，Suita）；H. Ohgushi（グループ長），M. Ikeuchi：産業技術総合研究所セルエンジニアリング研究部門組織・再生工学研究グループ；N. Tamai，H. Yoshikawa（教授）：大阪大学大学院医学系研究科器官制御外科学整形外科．

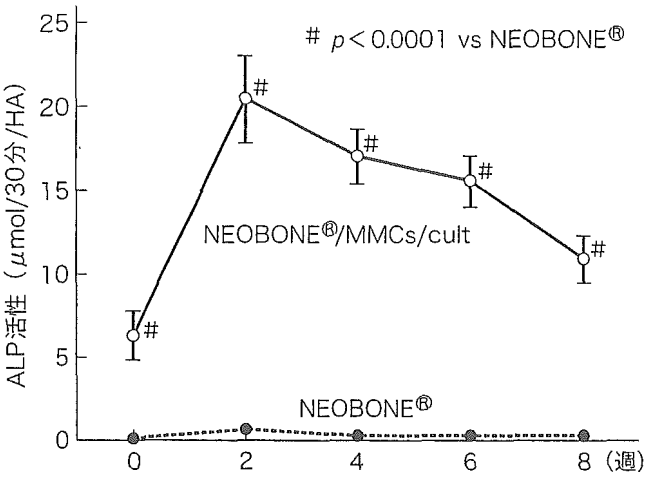

図2. NEOBONE®培養人工骨の *in vivo* でのアルカリホスファターゼ（ALP）活性．NEOBONE®培養人工骨（NEOBONE®/MMCs/cult）の骨芽細胞への初期分化マーカーであるALP活性は移植後2週目にピークとなり徐々に減少したが，移植後8週目でも高値を維持している．

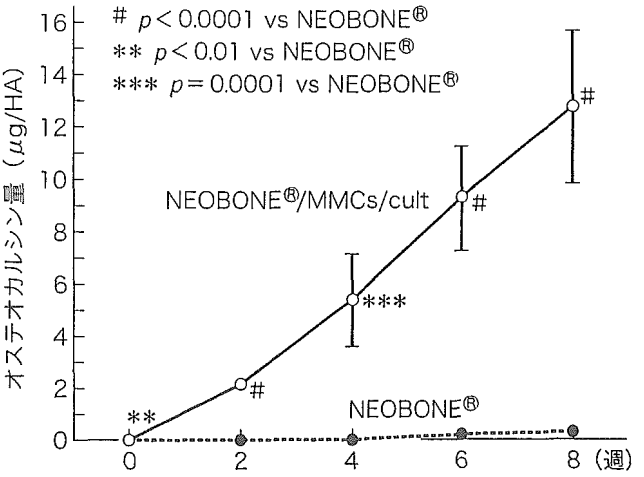

図3. NEOBONE®培養人工骨の *in vivo* でのオステオカルシン量．NEOBONE®培養人工骨（NEOBONE®/MMCs/cult）の骨芽細胞への後期分化マーカーであるオステオカルシン量は移植後経時的に増加している．

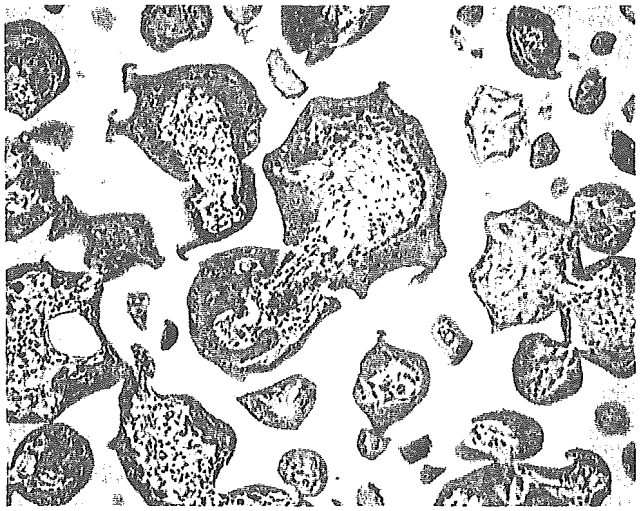

図4. NEOBONE®培養人工骨の移植後2週目の組織像（HE染色，100倍）．気孔内に骨芽細胞による活発な新生骨の形成が多数観察される．

Ⅱ．培養人工骨の生化学的分析

骨芽細胞への初期分化マーカーであるアルカリホスファターゼ（ALP）活性をNEOBONE®を担体とした培養人工骨（NEOBONE®培養人工骨）で測定したところ，培養7日目から高値を示し14日目の培養終了時まで維持された（図1）．その後ALP活性はラットの皮下移植後2週目にピークとなり徐々に減少したが，移植後8週目でも高値を維持した（図2）．また骨芽細胞への後期分化マーカーであるオステオカルシンの含有量は移植後経時的に増加した（図3）．以上より，NEOBONE®上にて培養分化誘導されたMMCsは骨芽細胞へ分化したことが確認された．

Ⅲ．培養人工骨による生体内での骨形成

図4は本来HA単体では骨形成が生じない皮下への移植後2週目のNEOBONE®培養人工骨の組織像である．NEOBONE®の気孔内に骨芽細胞による活発な新生骨形成が多数観察され，培養人工骨の骨形成能が証明された．また図5aは移植後8週目の組織像であるが，新生骨や骨髄細胞がほぼすべての気孔内で観察されたのに対し，ほかの日本の合成多孔体HAを担体とした培養人工骨は不十分な連通多孔体構造のためわずかな骨形成しか示さず，まったく組織侵入のない気孔も存在した（図5b～d）．以上の結果は骨再生組織工学の担体としての多孔性HAにおいて，NEOBONE®の有する連通多孔体構造の重要性を示している．

Ⅳ．培養人工骨内新生骨の三次元評価

培養人工骨中の新生骨量の定量測定のためにマイクロCT分析を行った．前述の組織学的分析はサンプルの切断面レベルにより結果が異なり，サンプル全体の骨量を正確に反映しない．この点マイクロCTは三次元構造を再構築することができ，新生骨の三次元分布やサンプル全体の骨量を測定することができる[12]．図6aは移植後8週目の培

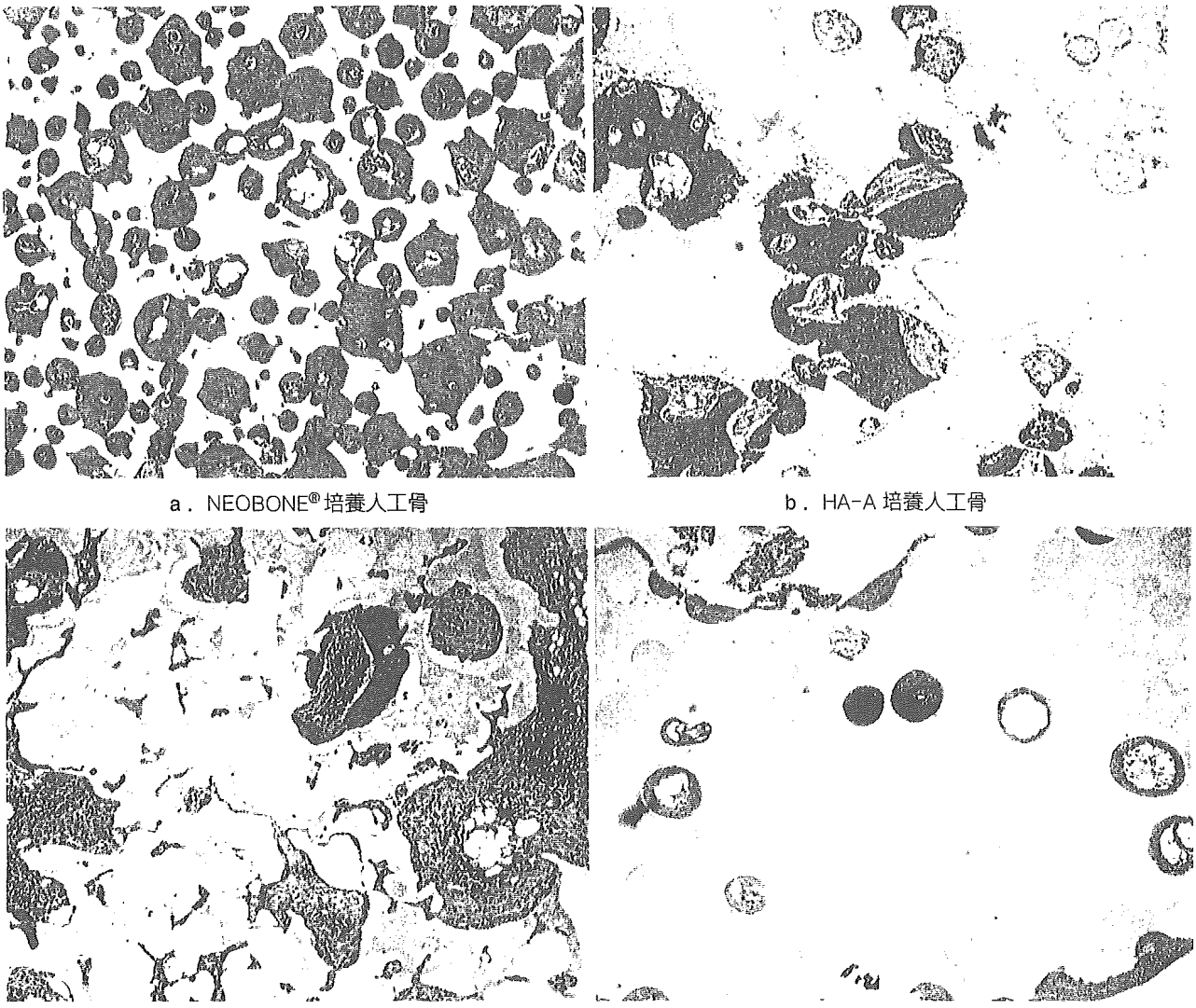

a．NEOBONE®培養人工骨　　b．HA-A 培養人工骨

c．HA-B 培養人工骨　　d．HA-C 培養人工骨

図 5．NEOBONE®培養人工骨およびほかの市販合成多孔体 HA 培養人工骨の移植後 8 週目の組織像（HE 染色，40 倍）．NEOBONE®培養人工骨ではほぼすべての気孔内で新生骨が確認されるが，ほかの市販合成多孔体 HA 培養人工骨はわずかな骨形成しか示さない．

養人工骨の組織像，図 6b はほぼ同部位のマイクロ CT である．マイクロ CT はグレースケールで表現されるが，これを組織像と比較して閾値を決定することにより HA，新生骨（NB），軟部組織（F）を区別することができる．コンピュータソフトにより中間色の新生骨領域を図 6c のようにオレンジ色に変換した．

移植後 8 週目の NEOBONE®培養人工骨中央での新生骨の分布を評価した（図 7）．白い部分はアパタイトで，オレンジ色は図 6 で示した新生骨である．表面だけでなく中央の気孔内にまで新生骨が確認された．次にこのオレンジ色部分の体積を新生骨量として定量評価した．図 8 に示すように，新生骨は 2 週目から検出され，期間とともに増加した．また，移植後 8 週目の HA-A，B，C の各人工骨を担体とした培養人工骨での新生骨量も測定したところ，NEOBONE®を担体とした培養人工骨よりも有意に低値であった（表 1）．

V．考　察

骨形成条件が不良な骨欠損の修復において，再生組織工学の手法を利用した再生医療には大きな期待が寄せられている．この手法は多孔体担体を必要とし，その担体は生体適合性と荷重下での骨格構造を支持するため十分な初期強度を要する．さらに細胞を導入するため三次元連通構造を必要とする．連通多孔体構造をもつ NEOBONE®の連通性および高気孔率は骨髄間葉系細胞などの骨形成細胞の導入